The Way of the Force: How Attractor Dynamics and Contact Coordinates Local and System Behavior for Multi-Agent Object Transportation

Benjamin Russ
Master of Science Thesis
Mechanical Engineering
University of Cincinnati

Committee:

Dr. Tamara Lorenz
Dr. Manish Kumar
Dr. Ali Minai
Dr. Nikita Kuznetsov

ACKNOWLEDGMENTS

Before diving into the fascinating world of robotics, I could not have completed this work without the wonderful support network around me. First, I would like to thank my wife Andrea who has been with me through every step of this journey. She has always shown me love, compassion, understanding, and notably shared excitement when my adopted robot children displayed their first movements. Next, I would like to thank my parents for their sacrifice to ensure I received a good education and instilled values which I hope to carry for the rest of my life. I would like to next thank my thesis committee for dedicating their time and effort to provide insightful comments throughout this process. Lastly and certainly not least, I would like to thank my advisor Dr. Lorenz. I am ever grateful for her supporting my curiosity and excitement for robotics while encouraging me to be the best researcher I can be. I forever treasure our insightful conversations about what the future might hold and sharing our experiences in this ever-growing world of science & engineering.

ABSTRACT

Multi-robot systems are a promising solution for object transportation as they have huge advantages over single-purposed robots - they are more versatile, less specialized, and more resilient to system failure while they can be scaled in numbers to meet operating requirements. As humans continue to explore further into our universe and domestic needs continue to grow with an increasing population, more robots will be required to complete more jobs. Most importantly, this current philosophy does not consider environments without human intervention or teleoperation. In projects such as NASA Gateway where "galactic pitstops" may not have a human aboard for many months, faults or incomplete tasks would endanger any mission relying on consistent uptime. Tasks such as moving a simple object from an initial position to a target region, such as staging materials, must be completed by a reliable robotic system to save mission critical resources and time.

However, when scaling numbers, multi-robot control and communication becomes complex as either monitoring technology or environmental cues must be deployed to enable coordination. In order to make the multi-robot system not only resilient, but also independent from environmental cues and hence universally deployable out-of-the-box, we propose a purely emergent interaction model based on touch between the individual mobile robots and contact with a manipulated object. This is realized with an attractor dynamics trajectory planner coined as "convergence" and a contact controller referred as "adherence" is benchmarked in a simulated non-prehensile object transportation task.

The outcomes from this project include the "convergence" and "adherence" algorithms and how they behave as a coupled dynamic system, a Gazebo and Robotic Operating System (ROS) simulation, documentation and analysis of emergent behaviors from the coupled dynamic system,

and finally exploring system patterns across a set of four predefined cases consisting of trials with one, two, three, five, and ten robots within the workspace. Ultimately, results show that the system is successful in moving an object to a goal position with different numbers of robots. However, the individual behaviors require further exploring into their exact impacts on the greater system performance.

Table of Contents

Tables

Figures

Variables & Terms

Variable	Description	Units
$\boldsymbol{\Delta X(t)}$	$Desired\ state - current\ state$	$-$
$\Delta \boldsymbol{F(t)}$	$Desired\ applied\ force\ reading - Current\ applied\ force$	$-$
$\boldsymbol{M_d, B_d, K_d}$	$Design\ impedance\ parameters$	$-$
$\mathbf{e}$	$p_d - p$	$-$
$\boldsymbol{\phi}$	$Agent\ heading$	$[deg]$
$\boldsymbol{\psi_p}$	$Goal\ direction$	$[deg]$
$\boldsymbol{\psi_r}$	$Repeller\ direction$	$[deg]$
$\boldsymbol{b_{nav}}$	$Convergence\ damping$	$[1/s^2]$
$\boldsymbol{k_p}$	$Stiffness\ to\ pushing\ point$	$[1/s]$
$\boldsymbol{k_r}$	$Stiffness\ to\ Repeller$	$[1/s]$
$\boldsymbol{d_p}$	$Distance\ to\ pushing\ point$	$[ft]$
$\boldsymbol{d_r}$	$Distance\ to\ avoidance\ point$	$[ft]$
$\boldsymbol{c_1, c_2, c_3, c_4}$	$Convergence\ Integration\ constants$	$-$

Equations

1 INTRODUCTION

How do robots become commonplace in our world of tomorrow? A world of home assistants, harmonious warehouse robots, and unmanned exploration into the depths of our universe. A world where humans and robots coexist. A world where we trust robots to freely interact with their environment without human observation or intervention. But what are we waiting for, why haven't we reached this utopian dream yet? With a history of injury and potential for great harm, precaution and hesitation are clearly warranted. However, in today's fast paced world, the need for robots to interact with objects and other robots within their workspace has never been greater. As manufacturers and suppliers balance between maintaining large inventory and supplying product just-in-time, autonomous systems (such as in **Figure 1**) must be scaled to match customer demands. At the final frontier, exploration will require resilient autonomy the further humanity desires to explore due to the natural limitations of the human body.

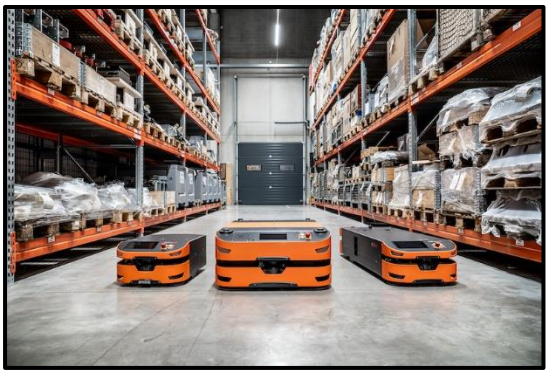

Figure 1. SafeLog AMR Logistical System

1.1 Motivation

With the dawn of the NASA Artemis mission and Gateway project upon us, humanity can no longer solely rely upon ourselves to fulfill our needs abroad and growing demands at home. Will we as humans ever see the outer reaches of our universe if we must construct and consistently maintain every galactic pit stop or "gateway" station? The only way forward is fully autonomous robots, resilient and free of necessary human intervention. Particularly mundane tasks such as moving objects are clear targets for autonomy. Some current examples are from space applications such as the AstroBee pictured in **Figure 2** and logistical offerings from Locus Robotics and Fetch

Robotics are clear advancements when applied in monitored spaces. However, these robots have limited versatility for object manipulation and applications beyond the International Space Station (ISS) [1]. In addition, these examples are well proven when teleoperated by a human or executing as a single autonomous agent. However, a limitation exists with this approach since performance and integrity of the system will be constrained to that single agent. Furthermore, a system of these agents each completing different tasks individually, in the same physical space, will likely sacrifice efficiency and/or performance compared to collaborative agents by virtue of allocated resources. However, for most robotic systems that share a workspace or attempt to actively collaborate, the motion profiles and decision processes have historically been rigidly controlled [2]–[5] and are rarely coordinated online. Therefore, we propose that new developments are required to enable active collaboration while improving flexibility, scalability, and resilience of Multi-Agent Systems (MAS).

Figure 2. AstroBee ISS Robot

1.2 Project Outline

To accomplish a resilient but performant MAS, a novel method completed in this thesis work is both an extension and new derivation of MAS research coined here as a Modular Multi-Agent System (MMAS). It should be noted that Multi-Robot System (MRS) and MAS or Modular Multi-Robot System (MMRS) and MMAS implies the same meaning throughout this work with the terms *"agent"* and *"robot"* used interchangeably. A *"modular"* system architecture in this context refers to two concepts. The first concept implies how the system allows for a robot to enter or exit a task within a workspace at any moment. This philosophy affords three major design points:

1. Many robots can fail while the remaining robots complete the task, provided enough are operational.

2. Robots can be reallocated across tasks as necessary to obtain better performance given environmental conditions.
3. No architectural limits to scaling the number of robots within a workspace

For these benefits to manifest, collaboration between the robots must exist to continue a task once a fault or potential "reallocation" occurs. In modern robotic systems, two choices are generally required to facilitate collaboration:

1. Source of information for each active robot in the workspace, decentralized or centralized. While a modular architecture could support both, the greatest benefit will be completely or mostly decentralized.
2. Communication between agents, either explicit (direct signaling) or implicit (indirect signaling).

Regardless of these decisions, communication amongst many agents operating in the same workspace quickly becomes complex. While collaborative systems have successfully demonstrated using (direct) wireless communication [6], significant limitations remain. A few of these notable limitations are bandwidth, vulnerable to interference and fragile processes too inconsistent to dependably recover from agent failure. Previous work targeting the solution of the communication problem have focused on optimizing the transmission volume through leader-follower architectures [7]–[9]. This "leader-follower" scheme relies on designating a "leader" robot with either increased capabilities or more information to direct "follower" robots through the given task. However, while identifying a leader in MAS may introduce architectural simplicity, it still suffers from a single point or process of failure. To avoid this issue, implicit communication, specifically touch, satisfies these needs.

Through interpretation of touch information coupled with available positional telemetry, collaboration on a common task in the form of an "assembled" structure of individual robots may arise. This leads to the second concept of the *"modular"* architecture which describes how the

robots contact and create *"emergent"* formations. Modularity is exhibited such that the robots will attempt to create and maintain contact with any external entity but can disengage at any moment. Furthermore, modularity is possible in this MAS since every robot is not required to find contact. Yet, contact between robots is designed as a desirable state, and encourages multiple clusters of robots-in-contact which may combine into larger formations while jointly moving towards a landmark or desired position. Given that the applied force created by the contact between entities is measured and recognized, we propose that a reactive behavior exists which maintains this contact.

For context of this thesis work, the robots being tested are omnidirectional, hexagonal-bodied, wheeled mobile robots operating within a two-dimensional, planar workspace. In addition, this robot will have discrete, planar edges which can create firm contact with external entities. While MMAS, as derived, is anticipated to be scalable to three-dimensional space and other types of robots, these are not tested in this work. The ideal "scenario" of MMAS is such that the robots operating within their workspace initialize and navigate to a landmark or desirable position (referred as goal position) along with other, identical robots. As all the robots *converge* to the goal position, distance between them will decrease and the likelihood for contact will increase. Once one robot detects contact with another robot, the heading of both robots will generally continue towards the goal position but *adhere* to the other robot. This ideally results in a heading which continues towards the goal position but is directed slightly towards the other robot. As the system progresses further, this interaction may multiply until the goal position is reached as a formation of individual robots. Once all robots arrive to the common goal position, a few consolidated formations will likely remain.

1.2.1 Object Transportation

To benchmark our proposed MMAS performance, we focus on a non-prehensile object transportation task, i.e. pushing an object from a known start position to a known goal position (further referred to as object transportation), see **Figure 3.** While the object transportation task has been extensively studied [6], [10], [11],we consider a novel solution based on only force tracking and resultant emergent formations that can jointly push the object. At system startup, the robots

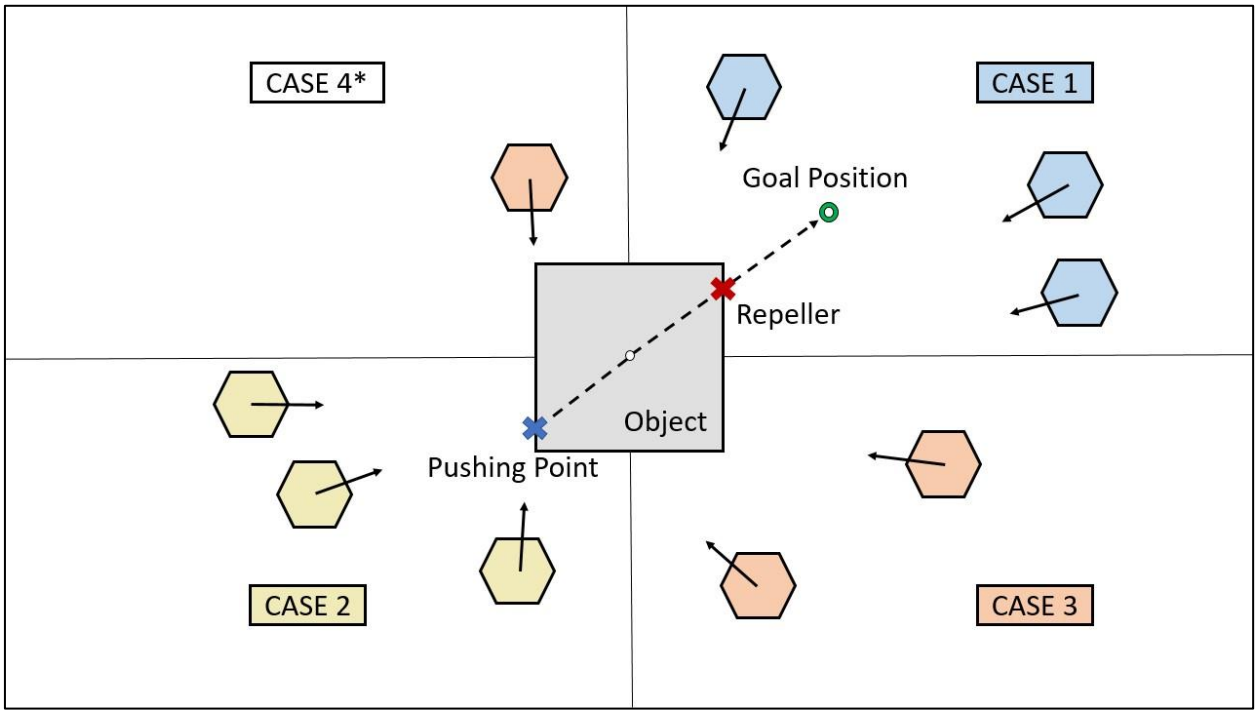

Figure 3. Illustration of the object transportation scenario. To demonstrate system performance, we consider four initial robot distribution cases: Case 1 (blue) - all robots are located on the same side as the goal position for the object. Case 2 (yellow)- all robots are occluded from the goal position by the object. Case 3 (red) - all robots initiate from a lateral position. Case 4 (all)- considers any robot initial position within 1-10m from the object center.*

are assumed to begin from random positions and are provided information about their own position, the position of the object, the object's geometry, and the goal position within the global frame. Importantly, no robot is aware of any other robot. Every robot is only tasked with moving the object. However, common in real world applications, it is assumed the object is too heavy for one robot to move on its own and encourages forming with other robots to move the object. The

objects' geometry determines an ideal *pushing point* which is gathered by each agent individually. This point is directly in-line with the center of the object and goal position and is always occluded by the center of the object, as illustrated in **Figure 3** (shortest linear trajectory). This pushing point represents the common attractor attached to the object for robots to *converge* onto. Additionally, to help the robots maneuver around the object to the pushing point a "repeller" is applied to the same line created from the object center to the goal position, but now it is always on the same side as the goal position. This is to prevent deadlocks and increase the likelihood for robots to apply force to the object at the pushing point. Then, as discussed above, contact creation and *adherence* between robots becomes more likely with system progression resulting in emergent formations.

Once the robots have *assembled* to this pushing point, they will begin pushing the object towards the goal position according to the location of the pushing point on the object. As the object is moved towards the goal position, the pushing point will be updated to remain in-line with the center of the object and the goal position as described above. Ideally, so long as the assembled robots push according to the pushing point, the object will have taken the shortest possible path to the goal position. During testing, four scenarios are conceived which are possible initial conditions for the MAS to encounter. Case 1 first initializes within the same quadrant as the goal position, Case 2 begins in the quadrant with the goal position occluded by the object. Then for Case 3, robots are randomly divided between the two remaining quadrants not covered in Case 1 or 2. Lastly, Case 4 allows for robots to begin anywhere in the workspace.

To successfully transport the object to the goal position, each robot is governed by two concepts coined in our project and defined in the following thesis as *Convergence* and *Adherence*. This architecture is intended to identify the two primary states of the robot, free and constrained motion. The *Convergence* subsystem dictates the real-time reference trajectory which guides each

robot to the pushing point attached to the object. This reference trajectory is generated according to a dynamic, mass-spring-damper relationship which is modeled after human locomotion. The reference trajectory is then passed to the *Adherence* subsystem which governs the behavior when contact is detected and generates a new heading based on a separate mass-spring-damper behavior from convergence. This new heading will be a slight alteration of the reference trajectory which will bias based on the reaction force from the incoming contact governed by a set of design variables.

1.2.2 Assumptions & Constraints

Through the creation of the MMAS, several assumptions are necessary and considered:

- The robot is mobile and holonomic, equipped with a rigid chassis with discrete surfaces for interaction.
- Each robot knows its wheel speed and has full control of its actuators.
- Each robot can measure and interpret contact forces measured and resolved to principal axes in the local frame. This haptic information paired with a force controller is used to support robots to maintain contact (with object and each other) while moving.
- Each robot knows its own position, the object's position, and the destination position for the object. There is no explicit communication between the robots and robots are not aware of other robots in the same workspace.
- Each robot can interpret or obtain prior geometric information of the object to establish the pushing point.
- Orientation of the object is not relevant. The goal position is reached when the object's center is within an acceptable tolerance to that location.
- One object to transport is present within the workspace and no other obstacles or objectives are considered.

1.2.3 Objectives

The following deliverables were promised for this thesis work as presented in the project proposal. With the exception of 3c, the following sections will illustrate all items promised have been completed and meet the expected standards set forth in the proposal.

1. **Cohesive movement model**:
    a. Nonlinear attractor dynamics as outlined in Warren and Fajen [12] implemented in this project for high level navigation. The derived model navigates to target positions and in future work, can be adapted to handle obstacles as well. This model will be completed by assuming target positions within the agent's task space and the agent's pose in the global frame is known to each agent.
    b. "Force Tracking" Impedance control is then implemented as contact handling or considered system "contact design". The impedance control will take the output from the above attractor dynamics and adjust as necessary to maintain the assembled body or push the target object. There are anticipated challenges regarding this development such as controller stability in the rapidly changing environment and tuning the dynamic parameters to the desired body forming behavior. However, it is expected with current knowledge of impedance control, this project's derivation is expected to produce a system capable of moving the object while creating a scalable framework for future developments.
2. **Simulation through the Robotic Operating System (ROS) and Gazebo physics engine:**
    a. Agents simulated with analogous mechanical structure and sensor outfit to a physical prototype performing the object transportation task. The agents are expected to start at random positions and converge towards the target. For this

implementation, the simulated agents will not require a calibration routine as a standard gaussian noise profile will be applied to the sensors. This is compared to the physical system which will require calibration for proper initialization. There are three metrics for success determined for this simulation. The first is whether the object arrives to the target position within a pre-determined tolerance. The second is the time to complete the given transportation task. Finally, is the cumulative path error of the object from the optimal path.

b. Creation of an analogous physical space in the gazebo simulator with scalable objects and comparable friction with defined boundaries.

c. Architecture of developed control software applicable to physical prototype in the ROS framework. This will promote repeatability between the simulation world and physical prototype while holding consistent development practices.

3. Physical prototype:

a. Improvements to the existing prototype from the previous senior design project [13] with sensor calibration protocols, initialization procedure, and complete documentation.

b. Validated testing suite and procedure for force sensors. This will include calibration, handling, operation within the system, and future improvements.

c. Movement accurate within pre-determined range and validated through video or other means. The path will not be pre-planned or hard-coded and will demonstrate the navigation capabilities of the system.

1.3 Thesis Outline

This thesis document is outlined according to five chapters of content which detail the work completed during this thesis project. While the final two chapters discuss the future direction for this thesis work and references cited throughout this document.

The first content chapter, “Background”, discusses current research for supporting topics which reflect the novelty and contributions of our MMAS. The next chapter, “Robots”, contains a formal description of the developed physical robots which the primary objective of this thesis work, the simulation, is modeled after. From there, the following two chapters discuss the concepts of convergence and adherence separately and when coupled as implemented for the simulation. These two chapters each detail the “Setup” and “Derivation” of each subsystem as it is applied to MMAS. Setup discusses any preliminary and specific assumptions necessary for either convergence or adherence. While the derivation is the detailed mathematical formulation which is ultimately the form taken within the simulation. Lastly, the “Simulation” chapter, completed as the primary objective of this thesis work, is discussed. First, the methodology and initial setup to test this system illustrates the differences between the simulated environment and physical application. Next, observations during the development of the system are recorded and represent the qualitative results from this work. Finally, the quantitative results of the overall system performance are presented following a separate analysis of the adherence system.

2 BACKGROUND

Before examining the complexities of the current project, several prerequisite topics have been demonstrated in the literature which reinforce the *Adherence* and *Convergence* concepts we have developed. First, the technical approach for convergence and its roots in attractor dynamics navigation are detailed. While navigation has been thoroughly explored in the mobile robotics literature [14]–[16], this chapter will first highlight how collaborative navigation in a MAS that allows for physical contact requires more attention in the field.

Secondly, this chapter aims to illuminate the methods for physical interaction which have been generalized between manipulator arms and mobile robots. While many examples from the field are derived for manipulator arms, we think this work provides a novel addition with a flexible framework for future development.

Finally, collaboration and scaling to more complex applications (i.e. additional robots, increasing objects within workspace, etc) and the associated challenges are discussed. While many researchers have relied on a leader-follower architecture, other avenues are explored which pose significant improvements for our MMAS.

2.1 Navigating Dynamic Environments

While navigation and swarm movements have been thoroughly documented, the concept of navigation while anticipating and accepting contact remains limited. In both single and multi-agent systems, researchers have generally opted for obstacle avoidance techniques which have classified touch as a fault or undesirable state. In the following review, several areas are explored which contribute to the derivation of convergence and the contained assumptions. Ultimately, the selection for one of these methods in a mobile robot navigation scheme depends on the available

information and the balance of computational burden. For example, Artificial Potential Field (APF) and Model Predictive Control (MPC) both present avenues to centralize for greater computational resolution and task efficiency at the cost of latency.

When robots are supposed to navigate within dynamic environments while executing simple tasks, the general problem is that while some information may be known such as the robot's own position and orientation, and the robot's destination position and orientation, other critical information such as the number of other robots or obstacles within the environment and their positions are not available. For our purpose, this requires that any robot moving through the environment should expect disturbances while continuing to complete the given object transportation task. Furthermore, while our approach does not consider obstacles, the robot cannot know for certain if the object is movable once contact is established. Since the heading to the object and to the destination is always known, APF is a prime candidate for allowing the robot to maneuver a complex environment [3], [17]. Traditionally, APF requires a desired position within an environment which then defines individual virtual force influences for any number of objects and agents within the robot's workspace. This force definition is governed by gains or tunable parameters which adjust the influence of forces from the obstacles and target. For example, [18] defines two separate gradients for approaching either a goal or an obstacle which combines into a single potential function that governs the heading of the mobile robot. The result is a local system which can navigate around dynamic obstacles which can be modified by key parameters to increase success rate and efficiency of the navigation task. While APFs have demonstrated great performance and flexibility for both navigation and obstacle avoidance, several drawbacks remain. The foremost is local minimum solutions which occur when the virtual forces are balanced, and a deadlock occurs. Since no motion is occurring, at least the deadlock robot is no longer participating

in the task. While our work can overcome the local minimum problem, we are also able to complete the task in the event given only a few agents are in deadlock. The other deficiency is that current developments do not clearly demonstrate collaboration on a task through direct contact between agents. While this could be developed, some practical limitations exist. The most apparent is the computational complexity which will increase greatly with the inclusion of more virtual forces. In addition, the field must account for every obstacle or goal within the designated range, as show in [18], for a proper heading which will increase the amount of required computational resources. As a result, a significant barrier will be reached to scaling down the size of any mobile robots or considering the efficiency of the system.

Another popular method for path planning the movements of multiple agents is MPC or in the case of MAS, Distributed Model Predictive Control (DMPC) [19]. This approach takes advantage of globally available telemetry and centralized computing to find the optimal path for each active agent while considering obstacle avoidance. Notably, this is done with an added prediction of the future state of the system. While the typically high computational cost, which scales with the number of robots involved, can be reduced as shown in Shen and Shi [20], DMCP still requires significant central intervention either in the form of global information or computation of the optimal state.

Machine learning approaches were also briefly considered for our development. The purpose for one of these learning methods in our work would be to broaden the success rate in more challenging environments with more obstacles either through optimization or to reinforce stability. In order for any learning method to be applicable for our context, training data would be required for weighted matrices or neural networks which would have to be translatable between the simulated and physical environments. Additionally, an optimality condition would have to be

devised which operates locally but results in a globally optimal solution for the overall system. For example, when coming into contact with another robot the trained subsystems would have to consider both maintaining contact and the most efficient path to the goal. The first method identified for this role is Iterative Learning Control (ILC) which considers minimizing the error between current and desired positions augmented by a trained weights matrix. One recent example is proposed in [21] where they introduced velocities to the optimization criteria. This was additionally paired with an Extended Kalman Filter (EKF) and Unscented Kalman Filter (UKF) to reduce sensor noise sensitivity. The result of [21] demonstrated better convergence and robustness to sensor noise than previous ILC methods. Another emerging option is Deep Q Networks paired with a vision sensor for navigation. An example application is in [22] which optimizes for all available actions to minimize distance traveled and avoid obstacles along the desired path. They found an increase in success rate and decrease in completion time with an increasing number of generations. While this section of the field is rapidly growing there remain significant drawbacks for our work which make the various methods challenging to implement. The first is that performance optimization is a costly endeavor which is often the target for these learning methods, is unnecessary for most mobile applications. Our work proposes that a "good enough" solution which completes the task may be a necessary concession to achieve a robust system architecture. In contrast, training a learning method for resiliency to increase consistency or handle edge cases within a workspace may be possible; but is not considered due to limited training data and lacking a clear transition to a physical system.

Finally, the trajectory planning method chosen for this work which complements the necessary disturbances originates from *dynamical systems* and a subsection of the field considered

attractor dynamics. This area attempts to harness the relationship between the stable behavior of balanced virtual forces and emergent or uncontrolled behaviors.

2.2 Contact Design & Control

In this section, the method to create and maintain contact between robots within a MAS is explored and divided into two major concepts, *contact design* and *contact control*. The term *contact design,* contrived for our purposes, is defined from established literature topics which describes the choices or constraints present that influence how applied force/energy should propagate and flow in an adherence system:

- Environmental Configuration
- Mechanical Design of the Robots
- Sensor Configurations & Processing

These topics are recognized specifically to highlight both the existing developments from the literature and identify the greatest impact to the performance of contact control. Following creation of contact between the robots, control is charged with maintaining it. While the bulk of research for this area focusses on robotic manipulator arms, many of these concepts transfer to mobile platforms. Traditionally, this is governed by a force controller which utilizes force sensor feedback to maintain a specific force value when interacting with a robot's surroundings. Rather, we are interested in pairing this with our prior design choices to focus on maintaining a stable physical connection rather than controlling a specific applied force value.

First, the force sensing method and how it is implemented onto the robot chassis dictates the accuracy and options to control force. For example, joint torque sensors are the most available option for industrial robots such as the KUKA LBR iiwa or FANUC CR-35iB. However, not every

implementation has a torque sensor at every joint due to cost while others may consider a load cell at the end-effector. In mobile applications, size and weight become considerable constraints and vary considerably. Most commercially available applications do not consider force sensing due to these limitations while researchers have found ways to effectively sense applied force for mobile platforms [23], [24]. In the instance of this project, the hexagonal shape of the chassis defines the possible system formations which would be different with other shapes or nonrigid chassis. By mounting load cells to measure force at the outer perimeter of the hexagonal robot, financial cost can be saved compared to torque sensors paired with motors. However, it is assumed that so long as the forces are resolved to principal axes relative to the agent then the developed adherence method is applicable.

Examples which have demonstrated different chassis and sensor configurations for interacting with dynamic environments can be found in [24]–[27]. These works each contain a different locomotion and sensing methodology but arrive at similar conclusions – namely that force sensing and its control is highly sensitive to disturbance. The most notable commonality from these examples is handling noise from the force sensor data. The most common approach to this problem has been variations of a low pass filter as described in [25]. The drawback to low pass filtering is computational delay from the filter's calculation and filter accuracy. When many physical interaction tasks require real time reaction, a computed filter may be detrimental. Which is why [24] trained a time-delay neural network to filter their force data which resulted in accurate calculation of point force along the outside of their shelled robot in same or less time than a Kalman Filter. Additionally, [27] demonstrated circumvention of force sensors altogether and rely on motor feedback voltage. The benefit to this approach is avoiding the cost associated with load cells or strain gauges but may be inconsistent between motors and mechanical designs.

Besides the sensitivity of the onboard sensors, the environment and its characteristics determine the necessary assumptions and imposed constraints on a mobile system. From the most constrained and efficient warehouses to exploring the vast, harsh surface of Mars, the operating environment introduces the greatest source of unknowns and variability when developing an interactive system. In an effort to simplify these spaces, we recognize two major assumptions for defining the operating environment for any mobile system, structured or unstructured. Generally, unstructured environments are unpredictable and fully dynamic. Some examples of robots in unstructured environments include undefined terrain as explored in [28] or search and rescue as demonstrated by [29]. These are common in nature or could be assumed when going between multiple structured environments that cannot be consistently monitored. Structured environments are often spaces, while dynamic, that have clearly defined patterns or boundaries which can be mapped or predicted with limited global or local information.

Our project assumes a structured, open and empty environment with only one object and other identical robots to anticipate contact with. This is critical as it allows us to assume that any contact one of the robots encounter is desirable and should be maintained. Consequently, obstacle avoidance and faulting are unnecessary for this work. Our contact design thus enables a collaborative workspace where contact is encouraged and a single, uniform objective is present in the system.

2.3 Dynamic Systems & Stability Considerations

At the intersection of navigation and interaction lies the study of Dynamics Systems. Our work has taken interest in this field for its application to real-time path generation and ability to handle dynamic environments with minimal information. However, stability is a concern in any dynamic

navigation scheme as the heading of the robot is no longer planned and is heavily dependent on the response determined by tuning constants with sensory and environmental feedback. Many of these dynamic system approaches take inspiration from swarming phenomena observable in nature, such as flocking of birds [30]–[32] or aggregation and rendezvous [7], [33]–[35] often recognized in insects.

Compared to some of the popular methods for navigation discussed prior, physical spaces are modelled as virtual forces mathematically defined as coupled nonlinear equations [36] in the dynamical systems method. We are using the term "virtual" to distinguish between a physical force applied to the body/chassis of the robot causing a disturbance and a virtual "force" influencing the robot's decision making. Traditionally, the sensory requirement for a dynamic systems approach is tracking the heading and distance to a goal alongside heading and distance to any obstacles. Often in this context, the virtual forces are acting upon the desired heading or path of the robot to steer either towards a goal or away from an obstacle. This may seem familiar to APF as discussed prior, but throughout this section I will illustrate how it behaves differently both in its outcome and its implementation.

The most abundant examples of dynamic systems navigation in the mobile robot field utilize attractors and repellers to reach their goal (commonly referred to as attractor dynamics). This is implemented through defining a distance and magnitude of effect which causes a robot to either be drawn towards a goal (attract) or deter away from an obstacle (repel). In our context, three criteria define a dynamical system which contrast it from other navigational techniques :

- A stable equilibrium point between virtual forces
- The applied process is continuous
- The main function can be evaluated for any point in time

By these definitions, APF would not fit as a dynamical system because a stable equilibrium point is undesirable and often classified as a "local minimum" in the associated publications.

Using dynamical systems approaches, [8], [37]–[40] demonstrates an effective MAS formation control scheme although through a heterogeneous architecture. In their latest work, [39], they demonstrate a system which can transport a lifted object through a system of fixed points, while they define asymptotically stable attractor states via heading direction and velocity. As a result of the compounding stable attractor states principle, while architecturally different, our work can expect similar resultant behaviors given the reliance on real time trajectories from a series of stable state attractors. Rather than planning many steps in the future and recalculating when a disturbance arises costing time and potential error, real time attractor states is a more robust solution and results in low computational cost, crucial for our scheme.

For our development, Fajen & Warren 2003 & 2007 [12], [41] and Warren 2006 [42] directly inspire the convergence trajectory planner with their attractor dynamics model of human locomotion that allows for avoiding obstacles and reaching a goal position. While using such a model will be beneficial to allow for applications in environments where humans and robots mingle, the flexibility for changing the dynamics of motion with minimal required information additionally results in a motion profile that eases into contact with the object in a smooth approach, which promotes a stable formation compared to sudden directional changes that are possible (and typical) in omnidirectional holonomic platforms. While our contribution is intentionally a second order implementation, there exist many other first order implementations that demonstrate similar outcomes [40]. However, Fajen & Warren [12] expressed that since a physical system contains mass, the modeled path was more true in second order form compared to the first order.

There are two primary drawbacks with a dynamic system reference trajectory approach. The first is the amount of obscure tuning parameters which provide flexibility to available behaviors at the cost of time to explore the many tuning combinations. The largest concern, however, is stability. In the case of dynamic systems, stability is often not presented as binary. As discussed later in **Simulation**, a range of resulting behaviors from expected to large oscillations in controlled values or even unexplainable, emergent behavior can arise. The challenge is exploring the bounds of these dynamic systems which has been demonstrated in [43] when handling disturbances. While their findings largely apply to interaction control, their approach may also apply to navigation since the desired reference trajectory is directly impacted by the physical disturbance from the previous time step. They propose an energy tank method with selective energy dissipation to mitigate heading oscillations for our approach. However, they also implement a Lyapunov function which is used to find the conservative and non-conservative portions of their "virtual" energy storage. In the future, it is reasonable to think this virtual energy storage could be used as either an efficiency or stability analysis for the overall convergence and adherence system.

Once a robot has embarked on its task, the next driving questions arise: why would a robot need to touch something? What actions should a robot take when it has touched something? These have been central challenges since the early development of robotics and continue into modern applications. One field which highlights the contact problem is physical human-robot interaction (pHRI). Specifically, [44] demonstrates how a robot placed in the same workspace as a human should always expect contact when executing a common task. This is critical since the robot is not always able to precisely predict the actions of the human and the placement of their limbs to guarantee safety during the task. To provide a safe workspace, the force and dynamics of the interaction must be controlled simultaneously. Traditionally, this is fulfilled by a force controller

which is most popularly implemented as “switching” or hybrid force control as discussed in [45]. This method requires selecting an axis within a reference frame to control external forces. The controlled axis can then be changed or “switched” to another due to some stimulus/criteria while positioning is done from the other axes. However, problems have arisen from traditional force control such as stability of the controller, success of the task, or requiring impractical constraints when presented with dynamic environments and tasks. Some of these problems can be addressed with a Lyapunov analysis and a hysteresis-relay based switching approach, but much improvement is still available. As a result of these limitations, a derivation known as impedance control has become a popular method for alternative motion/force control.

Detailed in the work of Hogan [46], impedance control defines the relationship between effort and flow, or force and motion; as a second order, ‘mass, spring, damper’ dynamical system. Hogan expands this concept for any impedance control system to be valid which is the existence of impedances and admittances. An admittance receives force and results in motion is balanced by an impedance which receives motion and results in force. This analogy can be applied to MAS and to our contribution at multiple scenarios within the object transportation task.

First is the case in which one robot moves the object by itself. This would define the robot as an impedance while the object is an admittance since it requires effort from the robot for resulting flow of the object. However, this becomes complex when more robots enter the workspace. In the case which multiple robots are not in contact with the object, but with each other; they remain individually an admittance while the body they create acts as an impedance once in contact with the object. This definition holds since the force created at the physical interface between the robots impact their flow at a behavioral level rather than just mechanical. In

summary, relative to each other, each robot remains an admittance while the modular assembly of independent robotic agents acts as an impedance relative to the tasked object.

Modern branches from this work have developed many systems which build upon the original idea but have enhanced stability, response to disturbance, or force sensing and processing. The most notable development is through adaptive systems which focus on the dynamical parameters and how they can be adjusted online to transform the interaction with the environment. The result of this is stable interaction with differing materials, objects, or motions in the same workspace and is highlighted in [47]. The next discovery of "form finding" or "force tracking", as demonstrated by [48], involves an end-effector following a complex surface while maintaining contact at a precise applied force. In the case of [48] a model capable of following a moving target workpiece in an accurate and robust manner is derived. This is particularly relevant to this project as contact the robots will be creating is likely to be moving in any direction due to the holonomic nature of the robots. This "force tracking" derivation tends to appear interchangeable to adaptive impedance control, but there are generally differences in the stiffness parameter and error terms as illustrated in [49].

For these modern approaches to be possible, the ensuing stability analysis has been a source of significant discussion. At the helm is the concept of "passivity" of interaction. This is the criteria which governs that more energy cannot exit a port of interaction than is input [50]. The specific design of passive impedance systems set forth in [51] refer to classical linear control systems and the positioning of a system's poles. This analysis method is outside of the scope of this work but would be the next step for formal stable bounds of this system. However, where this system deviates is in the complex nature of a dynamical reference trajectory paired with indefinite DOF of the system. Where traditional stability analysis of manipulator arms relies on fixed or known

DOF to constrain their stability analysis. One path to modelling this system may lie in the availability concept from thermodynamics which describes the amount of useful energy in a system as discussed in [52]. Based on the tuning and observations from this work, in addition to [53], there must exist a set of stable boundaries for the dynamical parameters for any given moment this system is active. While a small range of the stable boundary may be desirable behavior, locating that stable range would greatly narrow the solution space of possible parameters. Finally, since this is a coupled dynamical control system, *convergence* and *adherence* cannot be treated independently in the context of stability. If one becomes unstable with infinite growth, the other will follow and the system will become unpredictable.

Based on these findings, a few observations have been made in our work. The first is that mobile robots can effectively implement haptic sensing and act upon that information. Next, impedance control maintains both force and motion which is critical in mobile applications. It is not desirable for stuttering or instability of the interaction which could arise by switching or focusing on one axis to control. Finally, the impedance controller can be reconfigured online to change the desired interaction with any external entity as shown in ‘adaptive’ or ‘force tracking’ derivations. As presented in [54] and [55], adaptive hybrid “force tracking” impedance control fulfills these constraints and is adaptable to the developed MMAS. Their work implements an idea derived from [56] which describes stiffness as an inherent property of the environment, which allows the impedance controller to be implemented independent of stiffness and positional error, relying solely on damping, inertial, and error terms. Thus, the derivation assumes stiffness is zero. As discussed later, this results in the robots within the homogenous system creating and maintaining stable interaction with external entities for this object transportation task.

2.4 Facilitating Collaborative Interaction

At the foundation, cooperation, coordination, and collaboration represent similar ideas. All of these concepts refer to interacting. However, there lies a significant difference in resulting behavior when in the context of MAS. While the literature uses these terms interchangeably to refer to a modality of agents contributing to the same task within the same environment; I find it important to clearly define the usage for our work to differentiate between direct and indirect communication schemes and their resulting solutions. First, coordination is interpreted to be the basic form of multi-agent interaction where movement occurs between the agents in a coordinated way using the same or overlapping space, but there is no contribution towards an assigned task within the designated workspace. In contrast, cooperation is an indication of each robot's ability to complete their assigned task in the presence of the other robots. This would not necessarily gauge how the task load is shared, but rather only that a task was completed together. Finally, collaboration represents working together, including the ability to act on feedback from the other agents to improve joint task performance. In the case of this work a physical conduit enables haptic feedback while other approaches may be based on visual information exchange, auditory communication, or other means.

One final distinction we make in our work is between planned or emergent collaborative behavior. Distinguishing between a complex and programmed behavior is often trivial in most single robot systems. However, multiple robots and their compounding behaviors become difficult to track as the system scales. Ultimately, the key question we must answer is "can the movement of the object be modeled from the properties of the individual robots?". Thus, we must consider the levels of abstraction from the robot unit to system level and how well the resulting behavior at each level can be modeled against the amount of corresponding complexity [57]. The primary

emergence property that exists in this system is how a formation is created and then maintained throughout the task. At the robot level, the motion profile is fully defined for both constrained and free motion which, given the values from the sensors, can be fully computed. However, what changes when applying to the system level is the DOF which cannot be easily measured or replicated at the robot level. With an indefinite DOF at the system level, the robot becomes highly sensitive and incomputable without defining the DOF. Thus, the system behavior will decouple from the individual behavior depending on the DOF and "emerge" into formation once the robots are in contact. However, regardless of the DOF, free motion will always reflect the convergence subsystem and could be described as "planned" or "programmed" behavior.

As common in robotics, inspiration from nature and human biology contains crucial insights for efficient methods for interacting with the surrounding environment. One of these is the concept of tensegrity as coined by Buckminster Fuller [58] which describes how system integrity of a structure can be sustained strictly through a balance of forces within pre-stressed members. While this was a simple analogy when it was published, examples of this phenomenon have been found at the most basic levels of biological cell structures [59] and now applied to robotic systems [60]–[63]. However, as explored in [64] there remains a more virtual or behavioral version of this principle expressed in coordination of human teams. Their theory is that the same force balanced members in pre-stress can be applied to the connection of information between agents acting within the system. Our work takes this question a step further with the coupling of behavior and physical robot interaction.

To develop a convergence method, as mentioned prior, the robot must approach the object in such a way that it can collide with other robots while continuing towards a pushing position on the object. Thus, the breakdown of motion should be a collective response to a common goal, the

path taken to a target position in an MAS, and the creation and preservation of a formation. One method in MAS literature for stimulus response to a common objective is flocking. This method for aggregating many agents into a desired area typically relies on environmental cues to successfully complete the given task. Some examples from robotics literature are found in [32] and [65] where light is used as a central environmental cue. There are also examples where the cues for flocking is task dependent and more neighborhood centric such as [30]. Their focus is on the robot's neighborhood and does not distinguish between a friendly agent and obstacle. While these works do not necessarily achieve the optimal path to complete their given task, they use the constrained resources and information available to each agent to construct the best possible path. Another comparable topic to flocking is rendezvous or aggregation to a common point or object of interest. The first example from [66], which describes a method for a mobile robot to meet up with a UAV for charging at specific points using optimization techniques for path planning of the mobile robot and positioning of rendezvous points. The two examples of flocking and aggregation illustrates a general principle which current solutions can achieve an optimal solution with central information and/or computation, while a more responsive and robust solution may exist locally when considering dynamic environments. However, this trend is shifting as computation power becomes denser and more mobile.

The final aspect of convergence is the ability for the system to create and maintain a formation. While the control and specifics of the contact between the agents are discussed later, the generated reference trajectory must have support for both moving towards the object while accepting contact and disturbance to the current trajectory. One area of interest from the literature is formation control. This topic covers the idea of many robots moving in a coordinated fashion either around an obstacle, or in the case of [6] to move an object. In [6], they consider the global

position of agents on the object to optimally push to the goal position and orientation. While they decided to control the center of the formation, some works such as [5] take a decentralized approach by utilizing distances to nearest agents and objects to hold formations. They noted issues when faced with significant disturbances, which would be a challenge to fully accept contact. In addition, they rely on a leader-follower scheme with pre-defined formation shapes to complete their obstacle avoidance task. While this is the most popular architecture for simplifying dynamic, multi-agent environments which defines a leader amongst a group of followers. Typically, these "leader/follower" schemes reduce a common problem in MAS which is overwhelming communication traffic when relying on explicit communication (direct signaling) rather than implicit communication (indirect signaling) for task completion [7]–[9]. However, this often results in asymmetrical physical characteristics and/or roles within the environment which is contingent on the leader's resilience, or the leader selection process, to complete the task. Some methods have attempted to augment or reduce failure modes in these architectures as demonstrated in [67].

Both methods presented in [5] and [6] illustrate two key points to consider for the development of this work. The first is that the sensory information on board each robot will significantly guide the means to achieve a formation and any compensatory methods will be necessary such as central computing or a heterogeneous architecture. The second is that both works fully commit their agents into the formation without considering how the system will progress in the event of a fault, completion of the given task, or to reallocate resources to a more desirable area of the workspace. This is a crucial topic as more agents are added with varying object sizes and masses in which central optimization becomes prohibitive, explicit communication creates significant interference, and leader/follower schemes remain architecturally vulnerable.

In the current state of robotics, tasks such as passing objects between end effectors of high DOF manipulator arms have commonly required pre-planned or highly constrained routines to allow for multi-agent contribution. This has historically resulted in rigid systems that are not coordinated online resulting in limited fault tolerance and adaptivity [2]–[5]. Our development has identified and developed a method to enable active collaboration while improving flexibility, scalability, and robustness by encouraging many agents to complete a common task. If more agents are available than necessary, then excess agents could fail or complete other tasks while the system still converges. This is exemplified in [6] which illustrates how collaboration, paired with a global optimizer, can increase system performance directly with the number of agents completing the same object transportation task. Notably in the design of this system is the balance of resilience, task efficiency, and performance of the MAS.

Another method for active collaboration but not explored in [6] is direct contact between the agents to complete their common task. By interpreting the forces and distinguishing whether the contact is with another agent or the target object, an additional layer of collaboration becomes available to the agents. Some demonstrations of completing tasks without explicit directives or sharing information over a network, known as implicit communication, comes from [68] and [39]. These publications both illustrate the strength of collaborative architectures built on implicit communication, while [68] specifically utilizes impedance control to transport the object. However, where this project will improve upon these works is that they both rely on leader-follower or heterogenous schemes with designed system imbalance. Rather, this project leverages the propagation of force information through rigid structures leading to the formation of homogenous formations.

As previously detailed, force control and force measurement can be used to initiate, stabilize, and control interaction with any external entity within an agent's workspace. Furthermore, with the ability to alter the dynamic parameters a robot could maintain this contact for long periods as demonstrated in "force tracking" impedance control. Theoretically, locally controlled agents could touch one another and form a single modular structure or many substructures depending on the initial conditions of the system and object destination. Since the internally propagated forces act as a medium for implicit communication, provided the system is homogenous and can equally interpret the forces within the structure, uniform decisions should be made to maintain the structure and continue towards the common goal position. Additionally, depending on the impedance parameters the assembly can either behave as if mechanically bonded or loosely moving together. This flexibility may be key to adjustments and tuning in future applications with multiple objects to transport and more robots to prevent deadlock.

3 ROBOTS

From a previous project completed to fulfill a senior design requirement [13], a physical robot was designed, constructed, and tested to manifest the ideas presented in this thesis work. The physical robots are designed to be rapidly prototyped and tested while closely resembling the simulation scenario. The prototype hexagonal chassis is entirely 3D printed and is assumed to be rigid with a side length of 127mm. This hexagonal shape is purposeful to leverage possible formations and a resolution of six edges to measure force. While other shapes are possible and may yield better results, this is chosen for simplicity of implementation and mechanical design.

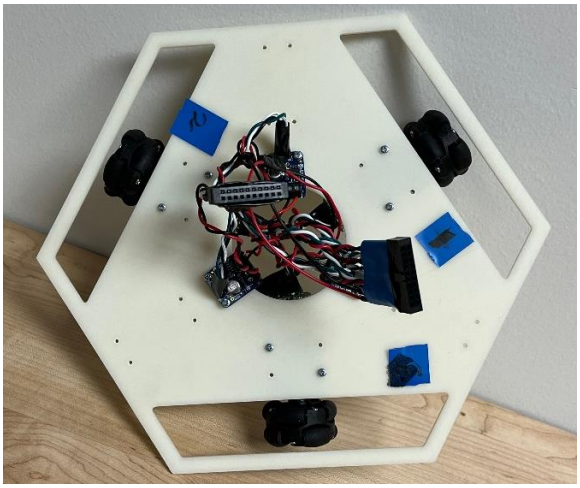

Figure 4. Lower "deck" of physical robot, power distribution and mechanical mounting

Load cells are mounted to the chassis around the perimeter and suspended facing outwards with no obstruction to the contact plate. The torques from the motors of one robot produce a theoretical maximum of 1.7-1.8kg applied force. Since the maximum applied force reading on the prototype is 5kg, the physical assembly can measure force from a maximum of three robots on the same axis while pushing an object. However, it is anticipated that more robots could be measured in this configuration when accounting for losses and slip in the omnidirectional wheels.

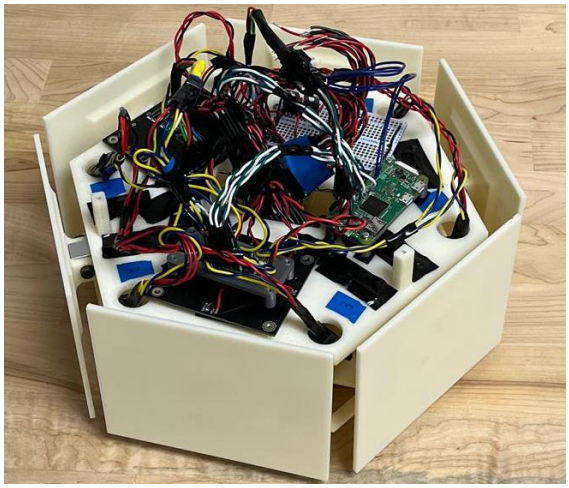

Figure 5. Upper "deck" of physical robot, logic and low voltage distribution. The load cells are mounted along the perimeter with the vertical plates attached.

The logic system for the robots is based on a high/low level architecture split amongst a raspberry pi and teensy. This architecture is intended to compute in parallel fashion which enables rapid sensor sampling, low latency forward kinematic calculation, and reduced computational load on the raspberry pi. ROS is chosen for high-level decision making and is compatible with the chosen hardware suite. The software package will include modules for UART communication, sensor fusion, actuation signals, localization, and behavioral dynamics.

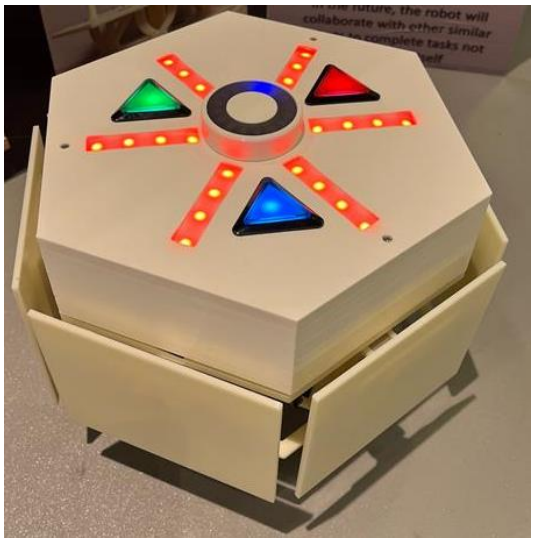

Figure 6. Fully constructed physical robot.

However, the physical sensors will require testing and accommodation to their manufacturer specification. When sample rate was considered previously for the load cells outfitted in the physical system, a rating of 10Hz is given by the manufacturer but could be increased to 80hz. However, increasing beyond 60Hz was found that the analog to digital converter (ADC) could not provide accurate readings [13]. In the future when a physical system is constructed, it will be crucial to test this sample rate and the accuracy of the output while observing differences in behavior. In addition to their maximum sample rate, sensor noise poses significant potential to create conflict with the simulation results. While outside the scope of this work, with a sensor fusion method such as an Extended Kalman Filter (EKF) or Unscented Kalman Filter (UKF), noise can be mitigated and physical behavior could more closely replicate the simulation environment.

When transferring from the simulated to a physical environment, several considerations are crucial to discern any differences in behavior. The first is that any dynamics simulator contains error inherent to floating point calculations. These may compound and influence behavior

differently than the microcontroller hardware outfitted in the robots. Next, the method in which dynamics is calculated within the simulation software may harbor assumptions or simplifications which do not accurately reflect either real world dynamics or the specific dynamics these robots may experience. This may especially arise from the force sensors implemented in the simulation which are axial torque sensors compared to the load cells mounted in the physical system. Thirdly, while the axis system is the same, as represented in **Figure 7**, orientation is not controlled in the simulation. This is currently a limitation of the navigational convergence system which attempts to hold a 0-radian orientation that aligns with the global frame. Finally, noise and interference are not considered since modeling the noise from the load cells is anticipated to be random due to electromagnetic interference.

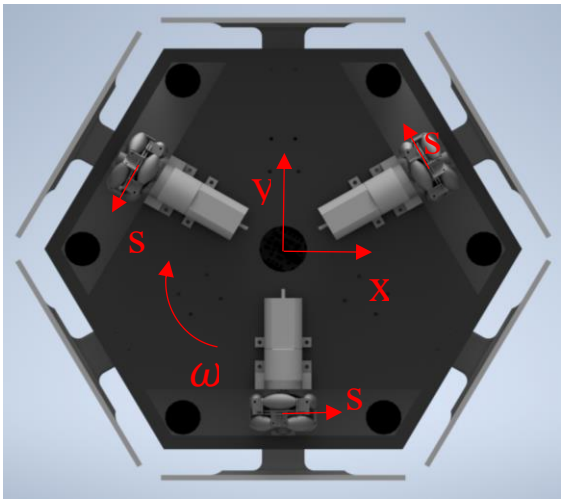

Figure 7. Coordinate system of simulated and physical robot.

4 CONVERGENCE

Considering that the object may be heavier than one robot can move alone, the robots must be able to work together in a synergistic fashion with other robots. While the goal is for the robots to join forces, the first step is for them to converge in one location. Henceforth, we call this part of the strategy *convergence*. Convergence allows for multiple robots to move in such a way that they arrive at the object at the desired "pushing point" and continue to the goal position. This implies that a robot can begin the convergence process from any location. Once a pushing process is initialized, each robot calculates a heading direction, and the robot begins moving towards the object. However, this may mean that the robot must maneuver around the object to begin pushing on a desirable side. Also possible, and intended, is that the robot encounters another, identical robot and makes contact. In both cases, convergence must provide accurate heading behavior to ultimately create a desirable, emergent formation of robots to overcome the object's inertia.

Following the foundation laid above, convergence is derived as an attractor dynamics approach to mobile robot navigation and congregation around an object for transportation. Using the available positional information, a lightweight, locally computed method which calculates a real-time trajectory is presented. This results in a navigation scheme which allows for physical contact and emergent formations. First, the assumptions and any prerequisites are detailed. Then, the formal time dependent derivation is presented. Finally, a proof-of-concept simulation is detailed to support applying it to the greater system.

4.1 Convergence Setup

Using the knowledge of the goal's position, the object's position and orientation, the object's geometry, and the robot's own position, each robot's primary mission is to approach the pushing point occluded by the object to the goal position. As illustrated in Figure 8, this is determined by the line directly created by the center of the object and goal position. Subsequently, this allows the robots to follow an "ideal path" or shortest distance to the goal position once pushing. To remain as lightweight and robust as possible, a nonlinear attractor dynamics solution, inspired by the work of Fajen and Warren [41], [69] and Warren 2006 [42] are adapted for real time trajectory planning. As discussed previously, this model uses the available information to create a reference trajectory which will be followed, ignoring any disturbances. As the robot approaches the object the influence of both attractor and repeller forces are acting upon the robot's heading. Both are necessary for this scheme to be successful as the robot will only attempt to reach the attractor through the object in the absence of a repeller. Simply put, this will guide the robot around the object until the pushing point becomes visible to prevent undesirable motion of the object. This repeller will act upon the robots heading from the closest undesirable point in the environment. In the case of this work, that would be the side which occludes the pushing point. However, in the future this could be the closest point to a dynamic obstacle or point to be avoided.

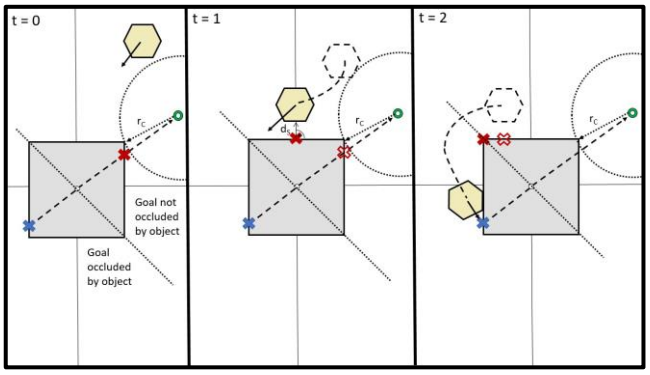

Figure 8. At initialization of system on left (t=0), the repeller begins co-linear with the goal position and center of the object. It then (t=1) transitions along the surface until the robot is on the occluding side between object and goal. Finally (t=2), the repeller remains a corrective force on the far corner of the object until the object reaches the goal position.

This repeller will continue to move along the object as the point resultant from the normal between the robot and the nearest surface of the object. The repeller will ultimately stop at the corner when the pushing point becomes visible as illustrated in Figure 8. Rather than overshooting the corner and wrapping around the edge, the corner will continue to steer the robot to remain with the attractor. Finally, once the robot reaches the pushing point, this must be inset into the surface since the update rate of the system will make the robot "think" it has reached the pushing position when the object may not have reached its destination. It is only a slight inset, but enough to prevent the robots from stuttering near the pushing point and smoothly pushing the object to its destination.

While following this "ideal path", each robot might physically contact another robot and the reference trajectory must remain stable. However, to maintain the created interface while progressing the task, the adherence model will utilize the reference trajectory and generate a final control trajectory that will feedback into the derived attractor dynamics model. While discussed in detail later, it is necessary to be mindful of this feedback when considering stability for both the current convergence model and any instability downstream that will impact the reference trajectory. As the goal is to assemble at the pushing point, the secondary mission of the robot is to stay connected with the fellow robot.

Finally, considering modularity in this MAS, once a robot has begun convergence onto the object it is impossible to enumerate all the possible faults and disturbances in a highly dynamic environment. For this feature to be applicable in future applications, it is considered as a fundamental behavior for the convergence model. By not committing to a path or dedicating significant resources to replanning an optimal path, this trajectory planner can handle changing the pushing position or completely different task in an instant. Additionally, since all robots tasked with moving the same object are likely to meet prior to the pushing point, clusters of robots should

form local neighborhoods of interactive behavior. The result of this is a highly resilient and potentially scalable system which does not rely on a small number of agents or processes to complete the object transportation task.

4.2 Attractor Dynamics Derivation

The convergence model is based on a mass-spring-damper system resulting in definable virtual attractor and repeller forces acting on the heading direction ϕ of each robot. The second order derivation proposed here,

$$\ddot{\phi} = -b_{nav}\dot{\phi} - k_p(\phi - \psi_p)\left(e^{-c_1 d_p} + c_2\right) + k_r(\phi - \psi_r)\left(e^{-c_3|\phi-\psi_r|}\right)(e^{-c_4 d_r}), \qquad (1)$$

requires the distance (d_p) and bearing (ψ_p) to a desired target position and the distance (d_r) and bearing (ψ_r) to an obstacle as input. The result is an attractor at the pushing point and repeller at an avoidance point as the output. Then, based on the remaining dynamic parameters k_p is the stiffness of the attractor, k_r the repeller stiffness, b_{nav} is the damping of the convergence system, c_1 is the attractor's decay rate, c_2 is the attracter fine adjustment term, c_3 changes the heading's approach to the repeller, c_4 is the repeller decay rate similar to c_1. The equation is implemented with imperial units such that distance is in ft and angular in degrees.

It should be noted that **(1)** is inspired from the work of Fajen & Warren, 2003 [12] and their attractor and repeller derivation of human locomotion. However, this project applies the motion profile rather than model it from existing behavior as done in their work. Additionally, similar assumptions are made here as in their work such as the model's inertia is zero. While an interesting future investigation may include a derivation with inertia and its effects on the convergence model.

While this framework is autonomous and implicit, the double integration method is a valid solution and converts the model into a usable, discrete form to determine the robot's heading value. It is understood that error will be introduced in this closed form function due to the discretization compared to the work completed in Fajen & Warren, but it is accepted, and attempts have been made to mitigate this error through idealized sensor sample rates. From basic integration where T is the sample rate of the system,

$$\dot{\phi}(t) = \dot{\phi}(t - T) + \ddot{\phi}(t) * T, \tag{2}$$

$$\phi(t) = \phi(t - T) + \dot{\phi}(t) * T. \tag{3}$$

The full solution for this project can be found in the appendix for reference. However, the final equation driving each robot's behavior is found below in **(4)** and **(5)** using the double integration method found in **(2)** and **(3)**. In terms of stability, top level analysis can generally profile this model without explicit analysis or location of bounds. However, adherence should also be included when performing an explicit stability analysis of convergence in this configuration since $\phi(t - T)$ is the previous output from the adherence calculation rather than the previous heading from convergence. In the future, it could be explored as a control problem whether the feedback coupling of the two dynamic models results in the best performance and stability.

With regards to convergence alone, the greatest concern is infinite growth since singularities do not exist. One countermeasure is to bound all input angles and output heading between $-\pi$ and π. This would largely prevent $\dot{\phi}(t - T)$ and $\phi(t - T)$ from dominating the solution and growing indefinitely. The other concern when employing a mass-spring-damper solution is oscillations within the defined bounds. The oscillation behavior should depend on

sample rate since greater time between samples will greatly increase the influence of measured inputs and increase difference from the previous heading value,

$$\dot{\boldsymbol{\phi}}(\boldsymbol{t}) = \frac{\dot{\boldsymbol{\phi}}(\boldsymbol{t}-\boldsymbol{T})}{\mathbf{1}+\boldsymbol{b_{nav}T}} - \left(\frac{\boldsymbol{k_pTe^{-c_1d_p}} + \boldsymbol{k_pTc_2} - \boldsymbol{k_rTe^{-c_3|\phi(t-1)-\psi_r|}e^{-c_4d_r}}}{\mathbf{1}+\boldsymbol{b_{nav}T}}\right)\boldsymbol{\phi}(\boldsymbol{t}) + \left(\frac{\boldsymbol{k_pTe^{-c_1d_p}+k_pTc_2}}{\mathbf{1}+\boldsymbol{b_{nav}T}}\right)\boldsymbol{\psi_p} - \left(\frac{\boldsymbol{k_rTe^{-c_3|\phi(t)-\psi_r|}e^{-c_4d_r}}}{\mathbf{1}+\boldsymbol{b_{nav}T}}\right)\boldsymbol{\psi_r}, \tag{4}$$

$$\boldsymbol{\phi}(\boldsymbol{t}) = \frac{\boldsymbol{\phi}(\boldsymbol{t}-\boldsymbol{T}) + \frac{\boldsymbol{T}\dot{\boldsymbol{\phi}}(\boldsymbol{t}-\boldsymbol{T})}{\mathbf{1}+\boldsymbol{b_{nav}T}} + \frac{\boldsymbol{k_pT^2}}{\mathbf{1}+\boldsymbol{b_{nav}T}}\left(\boldsymbol{e^{-c_1d_p}}+\boldsymbol{c_2}\right)\boldsymbol{\psi_p} - \frac{\boldsymbol{k_rT^2}}{\mathbf{1}+\boldsymbol{b_{nav}T}}\left(\boldsymbol{e^{-c_3|\phi(t-1)-\psi_r|}e^{-c_4d_r}}\right)\boldsymbol{\psi_r}}{\mathbf{1}+\left(\frac{\boldsymbol{k_pT^2}}{\mathbf{1}+\boldsymbol{b_{nav}T}}\left(\boldsymbol{e^{-c_1d_p}}+\boldsymbol{c_2}\right) - \frac{\boldsymbol{k_rT^2}}{\mathbf{1}+\boldsymbol{b_{nav}T}}\left(\boldsymbol{e^{-c_3|\phi(t-1)-\psi_r|}e^{-c_4d_r}}\right)\right)}. \tag{5}$$

Using the output from **(5)**, a reference x and y trajectory is created as a unit vector from the current position,

$$\begin{bmatrix} x_d \\ y_d \end{bmatrix} = \begin{bmatrix} \cos\phi(t) \\ \sin\phi(t) \end{bmatrix}. \tag{6}$$

This will be updated at rate T and is passed to the adherence model as a "reference" trajectory discussed below.

4.3 Proof of Concept

Throughout the tuning and testing phase for convergence a few notable behaviors were observed. The first occurred when applying the model to a one-dimensional Matlab visualization which illustrates the expected behavior when introducing a single repeller and a single attractor. To create this simulation, a theoretical motion profile of an individual theoretical robot to the attractor and repeller was generated which may be analogous to a real-world scenario. The first set of graphs (**Figure 9 - Figure 13**) demonstrates 12 different initial heading conditions ranging from -120 deg to 120 deg. With predetermined tuning values (Found in **Table 1** & **Table 2**), the heading angle correctly converges to the goal angle which represents the robot moving towards the goal.

Tuning values were achieved through a manual process beginning with the values initially presented in [12] until comparable results were observed. The important takeaway of these graphs is they follow a similar form as Fajen & Warren, 2003 [12] which demonstrates the discretized model derivation behaves analogous to the human locomotion model.

Next, after some initial testing in the Gazebo physics simulator paired with a backend in the robot operating system (ROS), a repeller was determined to be a necessary inclusion to complete the object transportation task. Notably, the robot would fixate to the given pushing point on the object. Often the result was robots pushing the object away from the goal or overshooting and never correcting. The next set of graphs, **Figure 14 - Figure 20**, represents adding the influence of a repeller. The primary concern when introducing this repeller is performance and stability. Performance now relies on the balance of these two tuning values to determine how the robot maneuvers around the object.

In the demonstrations below, an isolated system is illustrated with two scenarios. The first (**Figure 9 - Figure 13**), with an active attractor which converges all headings to the desired goal within ~0.4s without obvious oscillation. This most replicates the visualizations provided in [12] which demonstrates the model is reflecting the proposed model. The next (**Figure 14 - Figure 20**) is the same attractor definition with a repeller added. The additional virtual force resulted in a heading convergence closer to 0.7s but caused the heading to jump to avoid the obstacle at ~1.8s. The information from this data highlights a few key points for development. The first is that concerns of stability in attractor/repeller interaction remain valid and will require fine tune to achieve the desired “reference” trajectory behavior. The next is introducing the repeller makes this system initial condition dependent. Notice in the heading angle vs. time graphs for the attractor alone (Figure 9) and then following when the repeller is introduced (**Figure 14)**, the negative initial

headings converge differently than the positive initial headings. While it is logical the same path approached from different angles may require adjustment, further detail is provided later how different tunes will behave in the robots with full simulated physics.

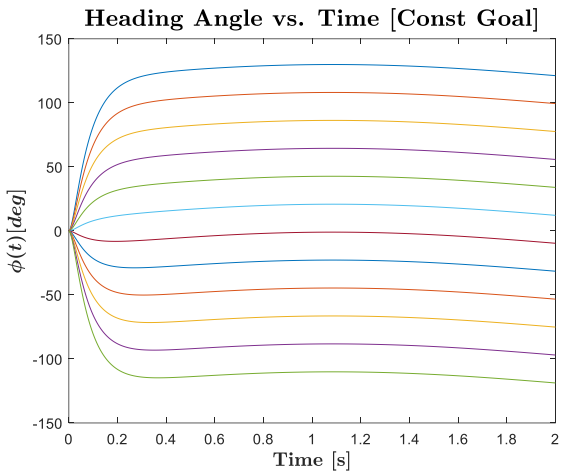

Figure 9. Scenario 1, no repeller heading angle vs. time

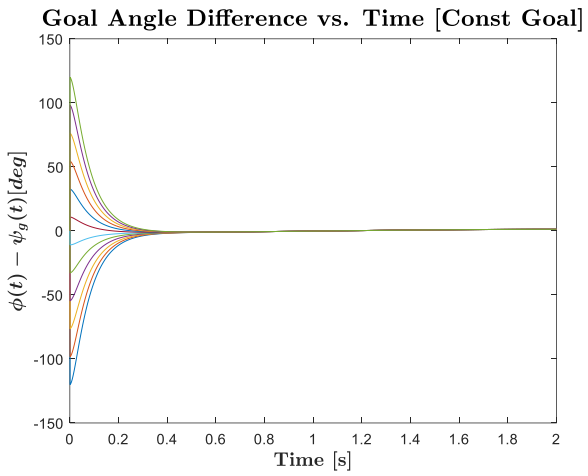

Figure 10. Scenario 1, no repeller goal angle difference vs. time

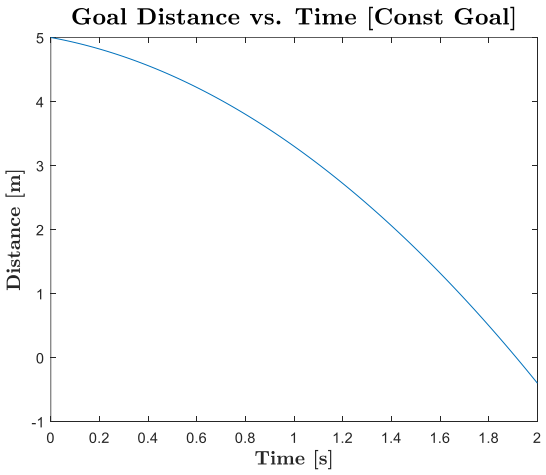

Figure 11. Scenario 1, no repeller distance to goal vs. time

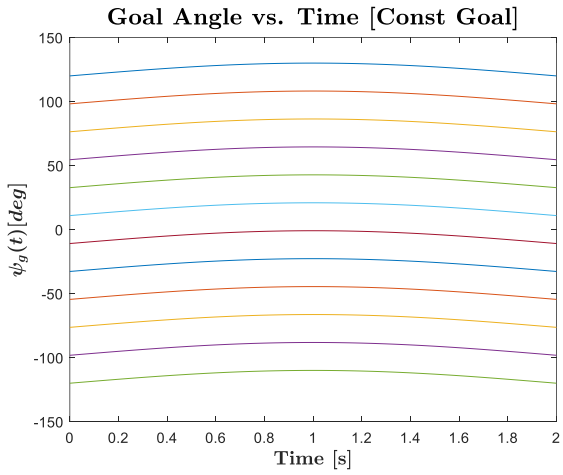

Figure 12. Scenario 1, no repeller goal angle vs. time

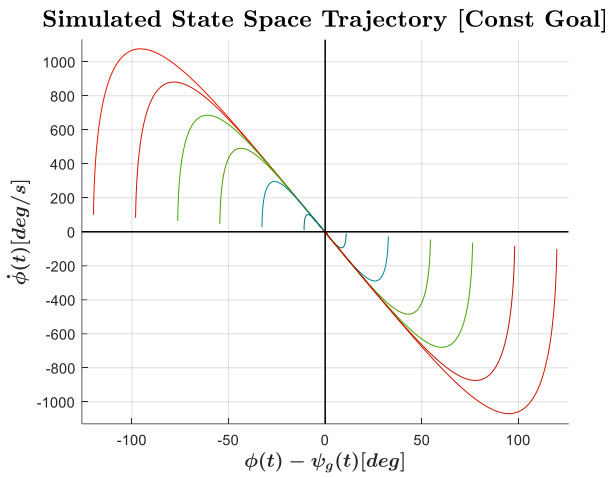

Figure 13. Scenario 1, no repeller state space

Attractor graphs (**Figure 9 - Figure 13**) generated with the following values:

Variable	Value	Unit
b_{nav}	80	$1/s^2$
k_p	1000.0	$1/s$
k_r	0.0	$1/s$
d_p	$-t^2 - 0.7t + d_p(0)$	–
d_r	$-3t^3 + 5t^2 - 0.5t + d_r(0)$	–
$d_p(0)$	5.0	m
$d_r(0)$	1.0	m
c_1	0.02	–
c_2	0.0	–
c_3	0.1	–
c_4	2.0	–

Table 1. Scenario 1 Convergence Values

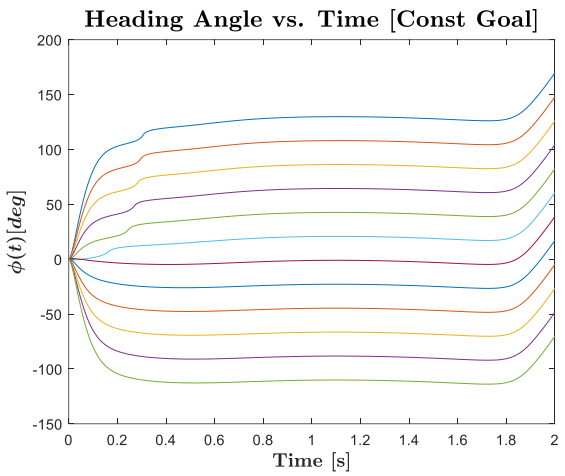

Figure 14. Scenario 2, repeller included heading angle vs. time

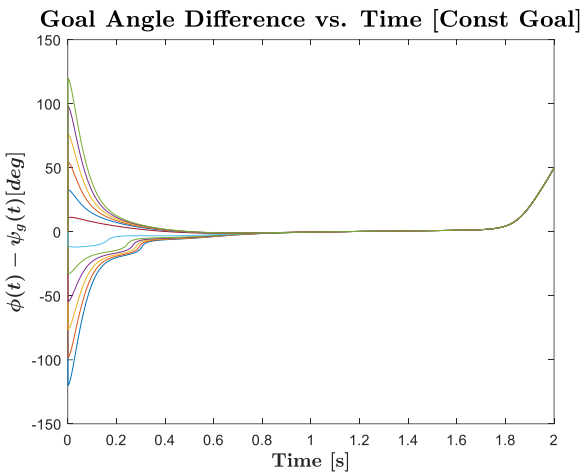

Figure 15. Scenario 2, repeller included goal angle difference vs. time

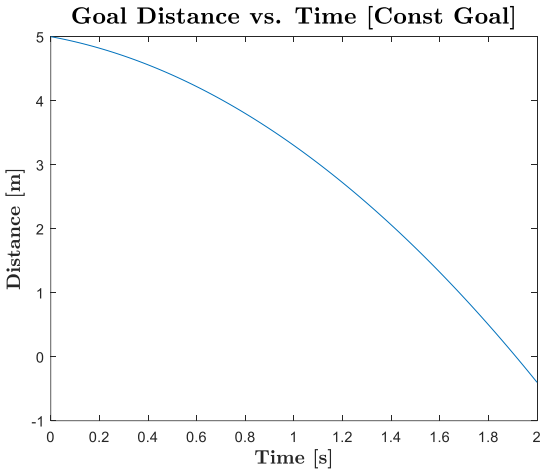

Figure 16. Scenario 2, repeller included distance to goal vs. time

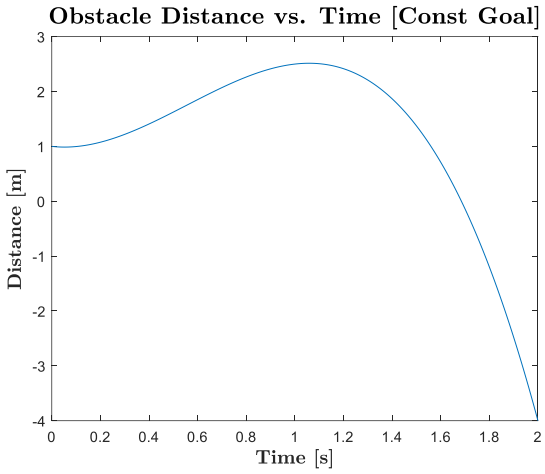

Figure 17. Scenario 2, repeller included distance to obstacle vs. time

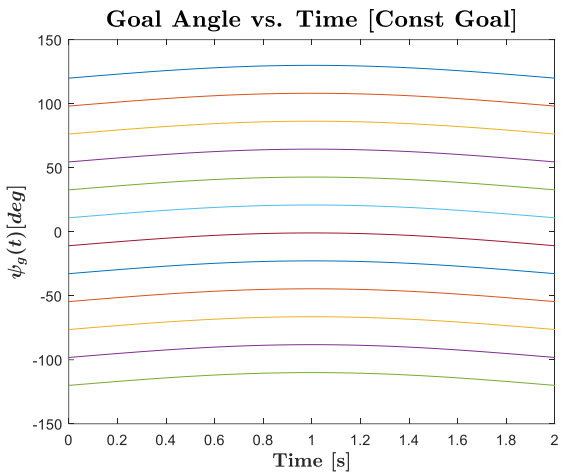

Figure 18. Scenario 2, repeller included goal angle vs. time

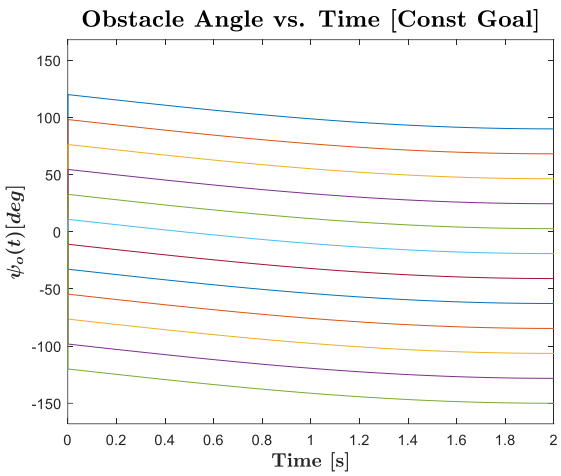

Figure 19. Scenario 2, repeller included obstacle angle vs. time

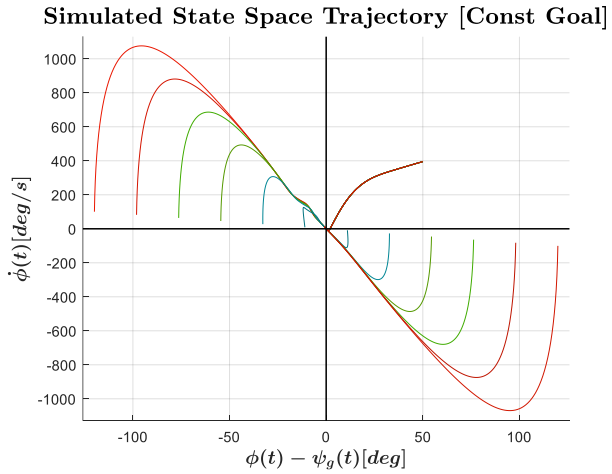

Figure 20. Scenario 2, repeller included state space

Attractor and Repeller Graphs (**Figure 14 - Figure 20**) generated with the following values:

Variable	Value	Unit
b_{nav}	80	$1/s^2$
k_p	1000.0	$1/s$
k_r	1000.0	$1/s$
d_p	$-t^2 - 0.7t + d_p(0)$	$-$
d_r	$-3t^3 + 5t^2 - 0.5t + d_r(0)$	$-$
$d_p(0)$	5.0	m
$d_r(0)$	1.0	m
c_1	0.02	$-$
c_2	0.0	$-$
c_3	0.1	$-$
c_4	2.0	$-$

Table 2. Scenario 2 Convergence Values

5 ADHERENCE

As time advances in the MMAS and convergence progresses, by nature of concentrating into a common region, the likelihood of contact will increase between entities. Assuming that this is either between agents or an agent and target object, leveraging this contact leads to a unique approach to collaborative robotics. The proposed solution, as detailed in this chapter, confirms that controlling and maintaining this interaction results in a modular structure comprised of mobile robots. In the context of object transportation, the benefits are clear such as efficient force application for a given object, resilience to faults, and agility between tasks.

Following thorough analysis of the literature, controlling both force and motion from a reference trajectory is best governed by Impedance control. Based on the presented behaviors, it is expected this method will remain true to the reference in free space and then slightly alter heading once in contact to control applied force while maintaining direction to the goal. In this section the necessary preprocessing, assumptions, and configurations are discussed alongside the final impedance derivation used for testing. In addition, stability and the necessary adjustment for a mobile system is discussed.

5.1 Adherence Setup

Impedance control has been conceptualized for decades in the field of robotics but was popularized and formalized by Hogan, 1985 [46]. Two major ideas were proposed in Hogan's work, Impedance and Admittance. These two concepts can be described by their relationship to effort (force) and flow (motion). In general, an impedance creates output effort from input flow and represents an active behavior which adds energy to a system. Whereas an admittance represent an environment which receives an input effort for output flow and absorbs the energy from an

impedance. In essence, an impedance excites an interactive system while the corresponding admittance will dampen the applied energy. In the case of our work, a single robot behaves as an impedance relative to the target. However, when two robots interact, they act as an admittance relative to one another by absorbing the energy from the contact and redirecting it into an altered trajectory. Then once the assembly collaboratively contacts the object, it behaves as a combined impedance relative to the object to push it to its destination. While this definition and model has guided initial developments, a more specific model is required for this work. One such derivation from "force tracking" impedance control provides insights for both regulating and maintaining contact with a desired surface.

By assuming stiffness is zero in the traditional second order impedance control scheme, a more stable and effective controller has emerged. Specifically, modulation of the damping term allows the controller to change how much to correct for incoming energy flow while remaining true to the reference trajectory. As discussed, this has been thoroughly demonstrated in manipulator applications but are lacking in mobile or multi-robot systems. However, a few commonalities exist between these two forms. The first is the filtering method. This project has chosen a first order low pass filter to remove noise from the force sensor readings. By adjusting the filter constant, the response time and accuracy can be balanced for the force sensor reading. In the case of the simulation, the filter was applied to torque sensor readings while the physical robots require the filter for each load cell around the hexagonal perimeter. The second commonality is in stability. While the mechanical structures are different, the dynamics of controlling the energy flow take similar forms. For example, proper sensor sample and control rates are crucial to allowing the updated trajectory to reflect the current state of the workspace and prevent large

overshoots to the next update. In addition, the inputs can vary from nonlinear oscillations to impulses which traditional impedance does not maintain stability and must be modified.

As a result of these stability issues, the derivation from Duan et al. [54] and Cao et al. [55] known as dynamic adaptive hybrid impedance (DAHI) control was developed. This implementation alters the damping term online depending on the control rate and current force readings in addition to assuming controlled stiffness is zero. This results in a behavior which can maintain a precise force following along complex rigid and even nonrigid surfaces in a traditional manipulator robot. However, for our purposes, precise force application is not a concern for the moment. Rather, we are interested in its ability to maintain a steady state and handle accumulating errors from environmental stiffness. Unique to this work is the interaction between convergence and adherence. While discussed in greater detail here, it is important to note the impact of the adaptive damping term before progressing. Since convergence is a traditional second order dynamical system, it has limited means of recovering from overshoots and avoiding singularities. Essentially adherence must stabilize the reference trajectory with the force readings to create a stable command trajectory. This coupling results in a dynamic system which can equally stabilize or enter chaotic instability.

During testing an additional challenge of deadlocking was discovered with multiple agents in the workspace. This behavior presented itself when the robots were in contact with each other and with the object. When near the pushing point the robots tended to push into one another in front of the point rather than combining their efforts to push the object as intended. In response, an F_{scale} term was added in addition to the other parameters to incentivize the robots towards the goal rather than into each other by uniformly scaling the amount of desired applied force (f_d). The

result of this parameter is if it is too large, the robot will nearly ignore the convergence reference trajectory and alter it to directly move to the pushing point.

To make this system possible, a few assumptions were made. The first is that the measured forces are resolved to principal axes prior to passing them into the adherence controller. The next is the sensor sample rate is high enough such it does not hinder stability. Lastly, the resolved force readings are accurate and timely for the state of the workspace.

5.2 Derivation for Physical Interaction within MMAS

The original proposition of impedance control from Hogan [46] describes the dynamic relationship between force and a difference of joint position for any DOF manipulator,

$$\Delta F(t) = M_d \Delta \ddot{X}(t) + B_d \Delta \dot{X}(t) + K_d \Delta X(t). \tag{7}$$

It is in the form of a discrete non-homogenous second order linear differential equation which regulates the applied force of a robot according to the applied dynamic parameters. Regarding M_d as inertia, B_d as damping, and K_d as stiffness with $\Delta X(t)$ representing the difference between current position and a desired position and finally $\Delta F(t)$ the difference of desired and measured force within the same frame as $\Delta X(t)$. The general interpretation of this equation is that setting a desired position "into" a surface, a dynamical response ensues to maintain a desired force.

For example, **Figure 21** [70] illustrates a physical interpretation of **(7)** in a 6 DOF manipulator arm. First, a "virtual", or in our context a "reference", trajectory is passed to the controller. In this situation the reference trajectory is "into" or "beyond" an object then a force interface is created. However "beyond" a rigid surface the reference trajectory lies, the strength of the force will change according to the predefined dynamic parameters. This force modulation

response will continue so long as contact is maintained and the relationship of true position and reference trajectory remains.

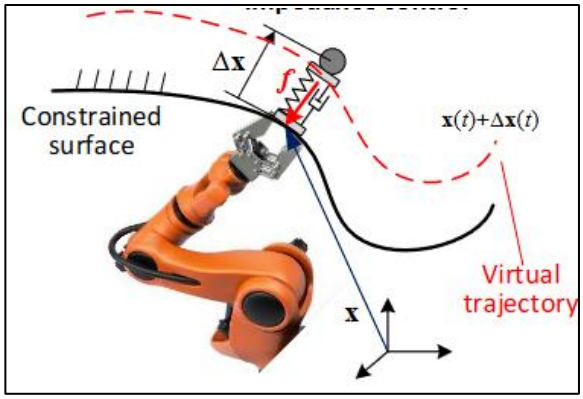

Figure 21. Impedance Control Physical Interpretation

The fundamental equation for this work as derived as **(8)** from Cao et al. [55]. It differentiates from **(7)** by assuming K_d is zero and modulating damping with an adaptive term, $\rho(t)$. However, **(8)** holds the same fundamental behavior described above but with wider stability bounds,

$$\Delta f(t) = m_d \ddot{e}(t) + b_d\big(\dot{e}(t) + \rho(t)\big). \tag{8}$$

Where e is a one-dimensional equivalent to $\Delta X(t)$ and p represents the current position relative to an axis and p_d is the desired position with respect to the same axis. In the case of this project, while a contact surface may not be continuous, optimal behavior will maintain contact to the desired surface through the entire operation and is modeled as continuous. Ideally, once the measured force reaches the desired, the system becomes homogenous and will attempt to maintain the contact and specified force value. While the same conditions remain from traditional control, the form of **(8)** promotes stability as a designed stiffness in the controller has proven unstable when tracking force along a continuous surface for extended periods. In our derivation, the surface is likely to be in motion and must be tracked for the entirety of the task.

As previously discussed, one challenge that arose during testing is the problem of deadlocks. This behavior originates from the balance of convergence and adherence systems where the resulting heading from adherence is directed into the contact interface rather than moving towards the goal while maintaining the interface. This problem was mitigated by adding a scaling

term, F_{scale}, to the desired force f_d. Since f_d is a unit vector in the direction of the reference vector F_{scale} will either force the command heading closer to the reference trajectory or more towards the contact interface. The revised form of **(8**) for our purposes is detailed as

$$(f_d * F_{scale}) - f = m_d\ddot{e}(t) + b_d\big(\dot{e}(t) + \rho(t)\big). \tag{9}$$

The adaptive term $\rho(t)$ modulates the damping of the system and is the primary means of maintaining stable interaction.

$$\rho(t) = \rho(t-T) + \sigma\frac{\big(f_d(t-T) - f(t-T)\big)}{b_d} \tag{10}$$

The behavior in **(10)** is accomplished by reacting to the online force gradient with a dynamic update rate,

$$\sigma = \frac{1}{e^{\alpha|\Delta f|} + e^{\beta|\Delta f'|} + U_{limit}}. \tag{11}$$

Where α and β are two control gains modulating the force error, Δf, and force error variation, $\Delta f'$. When σ is large, strong tracking compensation is exhibited, but produces large variations in contact force. When compensation is small, the tracking error will be larger, but the force measurement error will be small. An upper bound is applied in **(11)** to prevent infinite growth,

$$U_{limit} > \frac{m+bT}{bT} - \big(e^{\alpha|\Delta f|} + e^{\beta|\Delta f'|}\big), \tag{12}$$

$$U_{limit} \cong \frac{m+bT}{bT}, most\ applications. \tag{13}$$

Rewriting **(9)** in terms of $\ddot{e}(t)$,

$$\ddot{e}(t) = \frac{1}{m_d}\left[\Delta\hat{f}(t) - b_d\left(\dot{e}(t) + \rho(t)\right)\right]. \tag{14}$$

Where $\Delta\hat{f}(t)$ represents the scaled force difference,

$$\Delta\hat{f}(t) = (f_d * F_{scale}) - f. \tag{15}$$

Rewriting **(14)** in two-dimensional form,

$$m_d\begin{bmatrix}\ddot{x}_d - \ddot{x}\\ \ddot{y}_d - \ddot{y}\end{bmatrix} + b_d\left(\begin{bmatrix}\dot{x}_d - \dot{x}\\ \dot{y}_d - \dot{y}\end{bmatrix} + \rho(t)\right) = \begin{bmatrix}\Sigma f_x - (f_{xd} * F_{scale})\\ \Sigma f_y - \left(f_{yd} * F_{scale}\right)\end{bmatrix}. \tag{16}$$

Of which, the solution is found using the common double integration method,

$$\dot{e}(t) = \dot{e}(t - T) + \ddot{e}(t) * T, \tag{17}$$

$$e(t) = e(t - T) + \dot{e}(t) * T. \tag{18}$$

The final equation, written in one dimensional form,

$$\boldsymbol{e(t) = \left(-\frac{b_d * T^2}{m_d} + \frac{m_d}{b_d}\right)\dot{e}(t - T) + e(t - T) + \left(\frac{T^2}{m_d} + \frac{T}{b_d}\right)\Delta f(t) + \left(\frac{b_d * T^2}{m_d} + \frac{T}{b_d}\right)\rho(t),} \tag{19}$$

provides the desired command trajectory. This equation will not encounter singularities so long as the design parameters are set. Practically, this form remains simple to implement into a physical system since these are set design parameters, fixed control rates, or easily measured values such as position and applied force.

6 SIMULATION

Throughout this project, a method to visualize the combined convergence and adherence MMAS was needed to both validate and unify development for a future physical demonstration of this system. The Gazebo physics simulator paired with ROS was selected for its hardware scalability, publicly packaged libraries, and wide availability. The purpose of this simulation is to establish a proof-of-concept and collect success rate, performance, and scalability data. In the following sections a parallel is drawn between the existing hardware and the development of the physics and behavior simulation while illustrating potential next steps for this work.

6.1 Testing Methodology

To test system performance, we implemented our object transportation benchmark in the Gazebo physics and dynamics simulator, detailed in **Figure 3**. The simulation is paired with ROS and is derived from the "Open Base" project developed in [71]. For our purposes, we iterated upon the "Open-Base" architecture with multi-robot support, force sensor handling, multi-threading support, adherence & convergence subsystems, automated parameter iteration, datalogging, and general best practices among other changes. These features enabled benchmark testing of the conceived MMAS system according to the four cases designed to highlight the most common initial conditions the robots may encounter.

First, the environment is set up to resemble the physical environment of 20m x 20m usable, flat area with constant friction. The simulated robots have a regular, hexagonal chassis with a side length of 0.065m where the physical is larger with a side length of 0.127m. Both are equipped with a three-wheeled holonomic drive with the simulated robots achieving maximum rigid-body velocity of 0.67 m/s. The robots will always attempt to apply maximum torque and velocity.

However, materials and their stiffnesses are not accounted for in the simulation. This may have a measurable impact on the contact behavior as material stiffness is assumed to be existent in the environment and is not handled by the adherence subsystem. This requires future validation when the scaled physical system is completed.

For each sensor in this project, sample rate will contribute significantly to both resulting behavior and stability of the controllers. Since these are derived from autonomous systems, the hardware implementation must maintain as high a sensor rate as possible. However, the approach within the simulation is to increase the sample rate high enough so this is not the limiting factor to any robot behavior. Rather, any inconsistencies or abnormalities will lie with the base architecture or formulation of the system. In addition, sensor noise was not accounted for to increase consistency between trials. While this is not a realistic implementation it still requires accurate physics and dynamics which guide the simulated environment.

Next, the force measurement method is different due to limitations of the solver. The force is measured as torque from the wheel joints compared to load cells mounted around the perimeter on the physical robot. Since both systems resolve their applied force into the principal x/y axes, negligible differences are expected between the behaviors of the physical prototype and simulation and are assumed to be the same. A first order filtering method is applied to the sampled force data, although sensor noise is largely unaccounted for in the simulation. In addition it should be noted that the force sensors in the gazebo simulator should only be considered loosely in this behavior context. The exact force values are most likely not applicable to the real world since they rely upon mass and inertial values which may not reflect either the physical system or a realistic implementation. In addition, the simulation is configured such that the joints are velocity controlled and exact applied force is not determined within the simulation, only the speed which

the joints should be moving. There is a proportional relationship to applied force when speed is increased but the exact torque values from the joints are not controlled. The most likely outcome from this difference is an adjustment to the tuning parameters when applied to the physical system and will require future testing.

At startup, the desired number of robots are each spawned to a random position according to the desired case along with the center of the object placed at the origin. No other obstacle or other interference is included in these trials. Therefore, the geometric center of the object is to be transported roughly 4.24m from its initial position at the origin to a goal position of (3, 3) w.r.t. the global frame. Success is determined if the geometric center of the $1m^3$ (1m x 1m x 1m), 150g cube object is brought inside a radius of 0.3m to the goal position within a two-minute simulated trial threshold. It should be noted here that this two-minute limit may reduce the overall success rate compared to a higher time limit. However, this tight constraint is necessary for the sake of testing as increasing the number of robots exponentially increases the amount of data collected during the trial and real time required to run the simulation. One metric we closely observed during this simulation is scalability of the MMAS. In our context, scalability is determined based on successfully getting the object to the goal with a varying robot population. While a general change in success rate may not indicate a strong relationship, increasing the number of robots should improve other metrics accordingly such as faster completion time and reduced path length. In addition, more robots in a trial will increase system entropy potentially resulting in more sensitivity to oscillation and instability. However, this work is not focused on the exact values which the system is stable or chaotic and so a set of tuning parameters were decided for the entirety of testing. While this may not be “optimal”, it is intended to highlight the differences with more robots in the system and how the system handles an overall increase in available energy with the same response.

In the future, a more dynamic or learning based approach may allow for better response to scaling and increase system performance. However, this benchmark still completes our primary objective for a development platform to highlight emergent behavior of the conceived MMAS.

The four testing cases are defined as they may arise in practice, see also **Figure 3** in **Object Transportation**: In Case 1, all robots are initialized between the object and the goal position. This is theoretically the most difficult case since the robots will have to fully maneuver around the object before pushing may commence. In Case 2, all robots start on the occluded side of the object relative to the goal position, see also **Figure 8** in **Convergence Setup** for a definition of occluded space. This is expected to be the most successful case since the robots can immediately prepare to push with minimal maneuvering. In Case 3, the robots are placed lateral to the object. In Case 4, robots are randomly distributed within the workspace. These final two cases are anticipated to portrait the most realistic scenarios the system will encounter. For each case, 10 trials containing 1, 2, 3, 5, and 10 robots are sampled and averaged for performance assessment which is analyzed in the following sections.

Convergence Parameter	Value
k_p	1.5×10^9
k_r	6.25×10^{11}
b_{nav}	2.0×10^8
c_1	1.0×10^6
c_2	15.0
c_3	0.06
c_4	0.7
Adherence Parameter	Value
m	1.0
b	6.75×10^3
$alpha$	2.1
$beta$	0.32
F_{scale}	102.0

Table 3. Dynamic parameters used in testing, the four cases with 1, 2, 3, 5, and 10 robots across all trials.

6.2 Tuning & Observations

Throughout testing a few notable behaviors emerged along with significant observation of the tuning process. To choose the dynamic parameters for this system a manual process was implemented. First, adherence assumes that convergence is independently stable and provides an accurate reference trajectory. Additionally, we found during testing that while the chosen parameters for convergence may be independently stable, they do not hold once introduced to

adherence and must be re-tuned. Furthermore, since the two dynamic controllers are coupled, they did not behave as independent systems during tuning. For example, damping in either adherence or convergence often impacted both and any emerging system behavior. This was observed when stiffness in the convergence controller could begin oscillating and a change in damping of adherence could largely compensate and re-establish stability. Since the stable bounds of this system are transient, it is not reasonable to create an absolute min/max of the parameters and would require a separate controller. However, given that the sensors are reporting accurately and timely, the resulting *behavior* from instability of each parameter can generally be mapped. To prevent confusion and keep track of behaviors, one parameter was altered at a time only after sufficient observation.

Instability generally presented in several forms during the tuning process. The most notable is that the simulated robots would create an initial contact but quickly separate and head into seemingly random directions for an indefinite amount of time. Without an exact diagnosis of the problem, clearly the command trajectory overtakes the reference and settles into the undesired state without correcting. This indicates a possible local equilibrium of behavioral forces which may eventually be exited but rarely did during testing. Another unstable behavior was extreme oscillations of the commanded heading. This situation often resulted in the robot moving back and forth in place while touching and backing out of contact with an external entity. The behavior would most often perpetuate but could occasionally recover and resume the task. This was commonly diagnosed with greater damping either in the convergence or adherence method. With common forms of instability mapped, the bounds of each variable could be generally visualized. While obtaining the exact values is outside the scope of this work, each value was increased until these unstable behaviors arose at which the values were then tuned back. In the future, the exact

bounds of each parameter may be found through analytical stability analysis which may provide insight into an ideal set of values based on the current timestep.

6.3 Behavioral Case Study: Influence of Adherence controller

Before analyzing the system level data and outcomes, a case study of data from a Case 4 trial with two robots is analyzed. This is intended to illustrate the behavior of convergence and the downstream behavior of adherence more clearly in a simple workspace. As noted previously, since the two systems are coupled, instability within convergence does affect adherence and may not re-stabilize due to this relationship. Which is why this example provides the clearest behavior of the system rather than one with more active robots since instability grows with the number of DOF causing the data to become indiscernible.

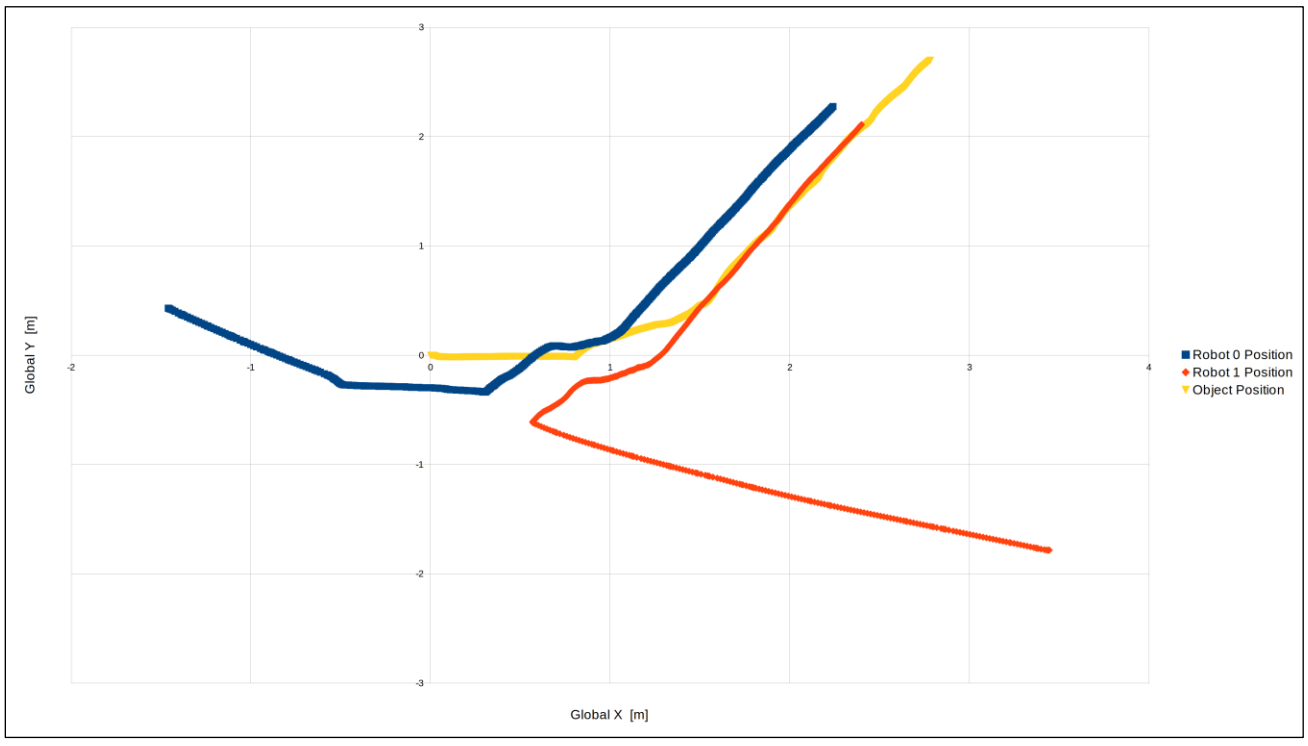

Figure 22. Robot & Object path over two robot sample trial period

Beginning with **Figure 22**, the robot's and object's path over the trial period is shown. From here we can roughly see the random initial positions of robot 0 at ~[-1.5,0.4] and robot 1 at ~[3.4,-1.8] with the object at the origin. Since the object is a 1m cube, robot 0 must first make contact with the object since its path is disturbed around [-0.5,0.25]. Following initial contact, robot 0 is able to begin turning the object until sometime later robot 1 is able to assist around [0.6,-0.6].

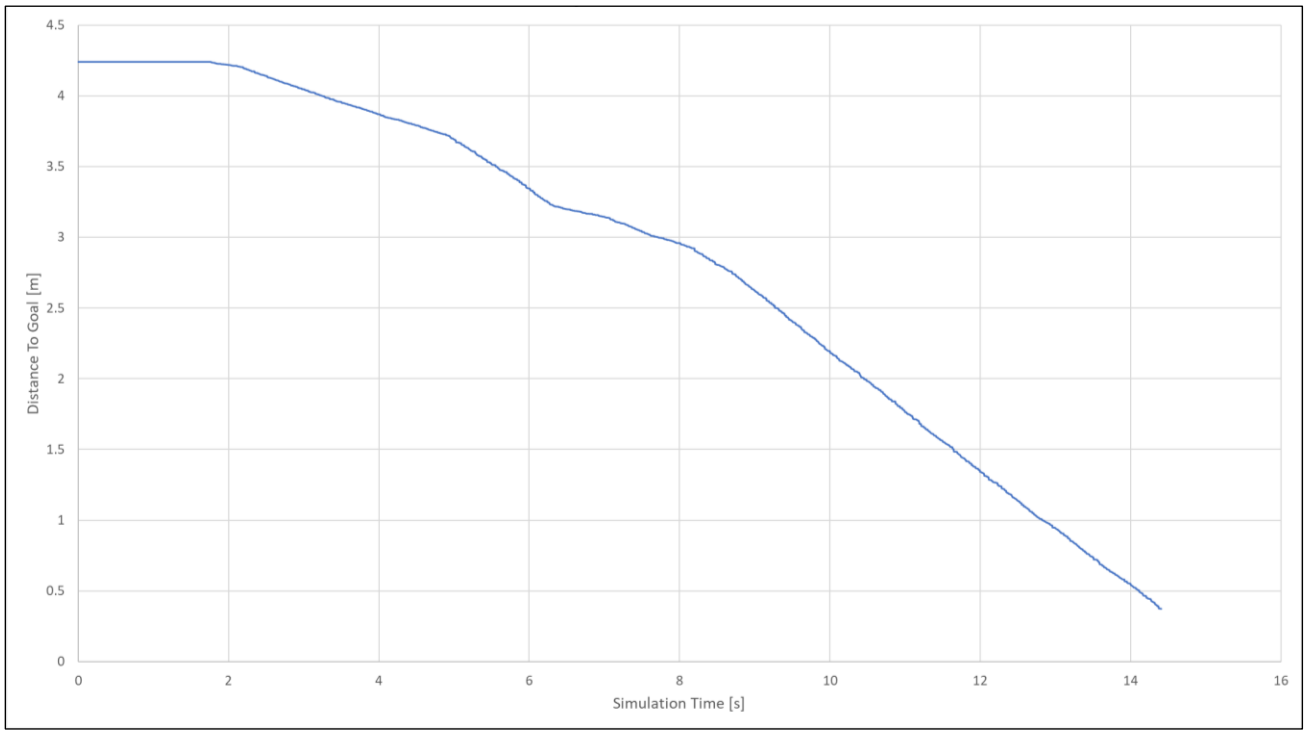

Figure 23. Object distance to goal during two robot sample trial

At which with combined efforts the pair pushes the object to its final position around [2,75,2.75] which is within the 300mm acceptable radius for the center of the object. Ultimately, the object followed a mostly straight, consistent path once both robots combined their efforts as shown in **Figure 22** and **Figure 23**, and completed the task in under 16 seconds.

While positional telemetry is important for a macro understanding of the case, the individual feedback and decisions of the two robots causing the object to be moved is more useful

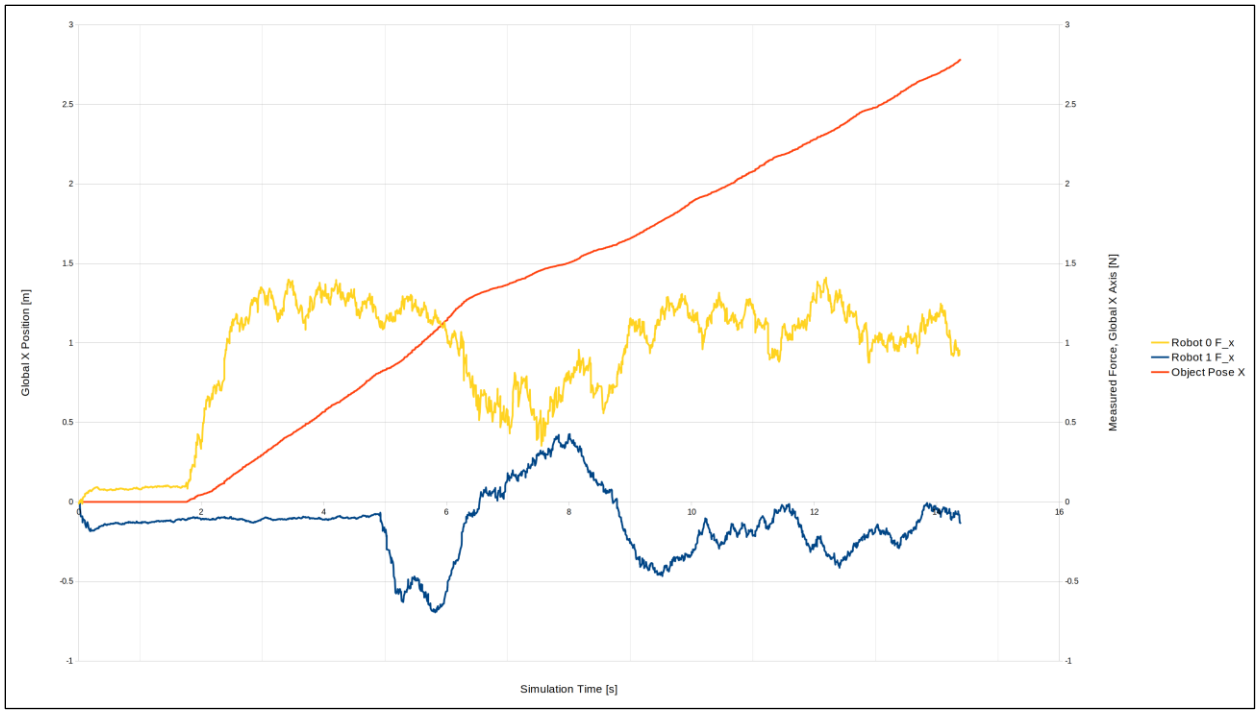

Figure 24. Robot 0 & Robot 1 measured force values in the global x frame compared with object's global x position.

to profile our behavior. As seen in **Figure 24** and **Figure 25**, a comparison is made between the position of the object and the measured applied force for each object divided into their respective global x and y frames. These figures additionally provide time stamps which indicate that the object first began to move around 2 seconds by robot 0 in the x direction as shown in **Figure 24**. We arrive at this conclusion since the x directional force by robot 0 at 2 seconds jumps from roughly 0.1N to settling around 1.1 – 1.4N until robot 1 arrives. The same procedure indicates that robot 1 creates contact with an external body around 5 seconds with the negative jump to roughly -0.5N of measured force. However, it is important to distinguish that this may not be direct contact with the object and may be with robot 0. While this would still apply force and accelerate the object, the formation would be different and ultimately control the object differently whether the newly applied force is to the object or the other robot.

Switching axes in **Figure 25** reiterates a similar message conveyed by the x axis data shown in **Figure 24**. However, movement in the y direction does not occur until robot 1 makes contact at

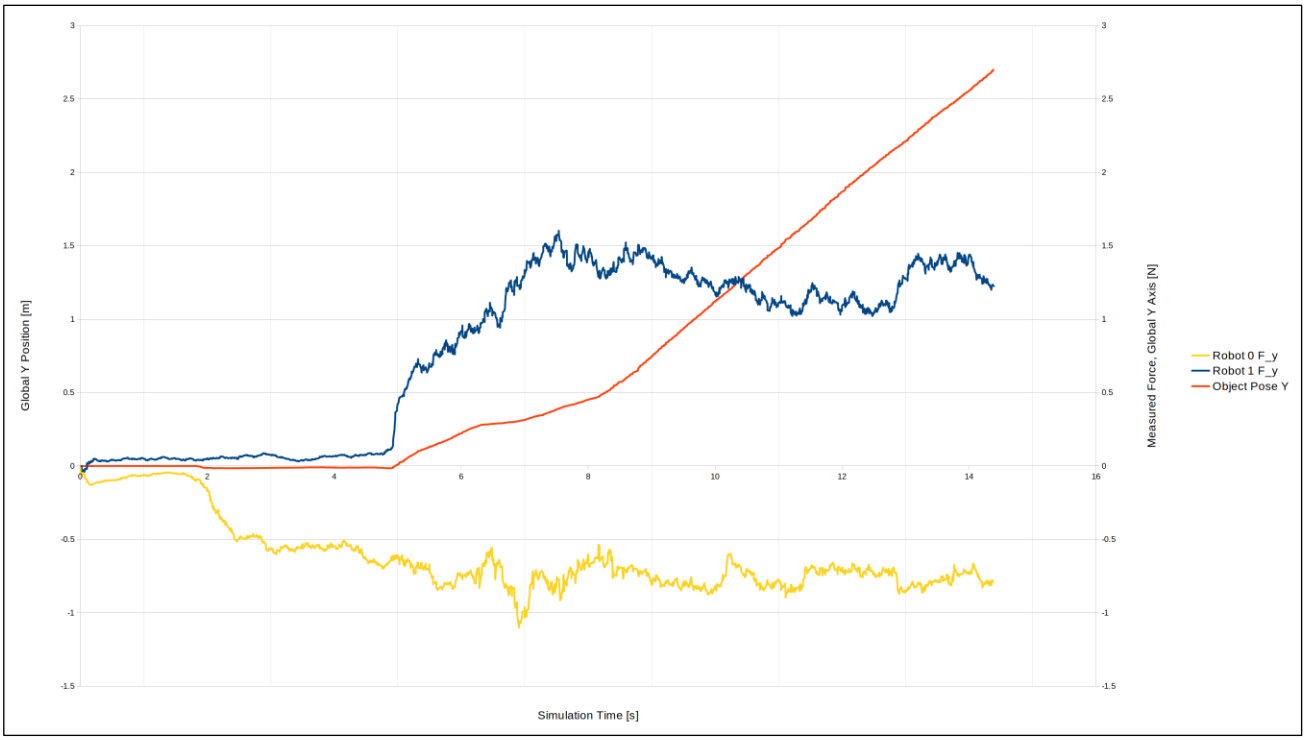

Figure 25. Robot 0 & Robot 1 measured force values in the global y frame compared with object's global y position.

roughly 5 seconds when the measured force quickly jumps to 0.75N and increases from there. This is compared to robot 0 making first contact at roughly 2 seconds and jumping to -0.5N of measured force but unable to move the object alone.

In addition to the sensory data, the convergence and adherence subsystems are utilizing that feedback in free space and then during the contact with both the other robot and the object to decide a final control heading. The effects of the changing workspace and the feedbacks into the output of the reference and altered heading is found in **Figure 26** where "Robot 0 Reference" is robot 0's reference heading, "Robot 0 Altered" is robot 0's altered heading with the remaining two similarly for robot 1's reference and altered heading. Three important behaviors are notable from this trial. The first is the offset of the altered trajectory from the reference created once each robot has contacted the object around 5 seconds of elapsed trial time. This offset occurs as a function of preset dynamic terms responding to the measured force values according to **(5)** and **(19)**. This

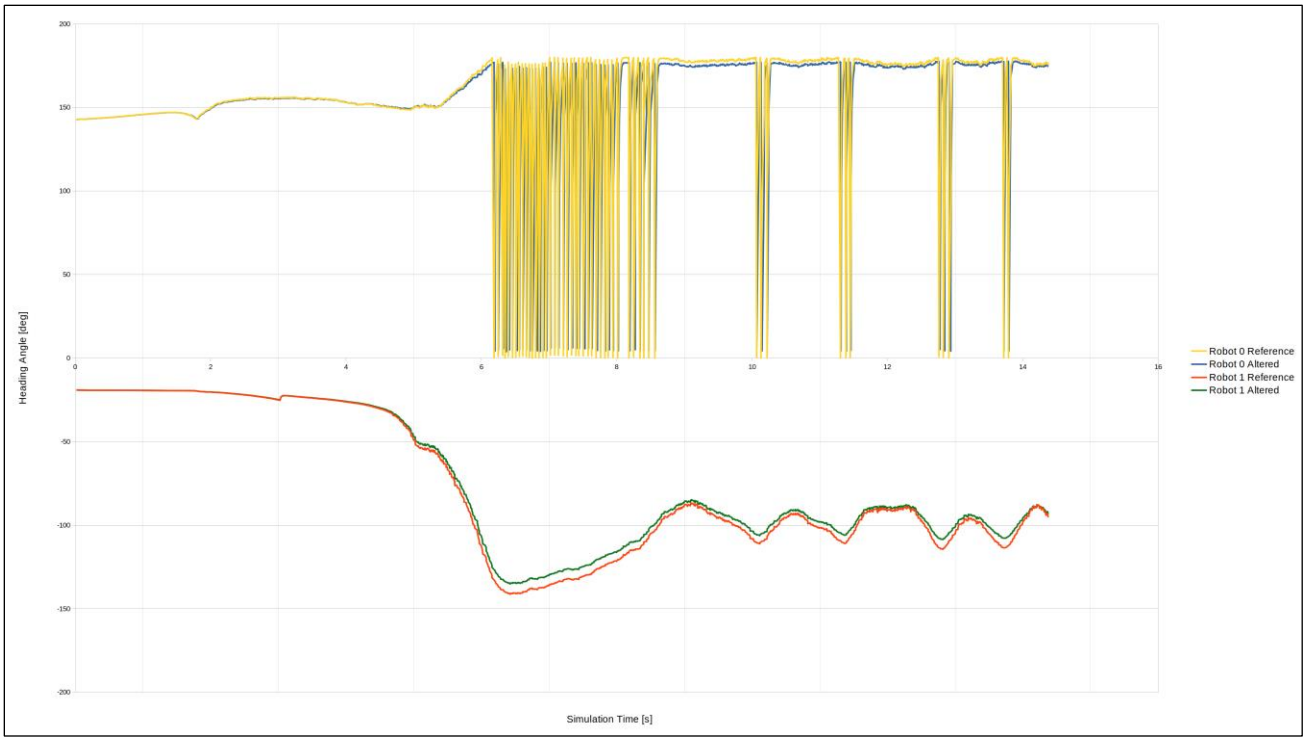

Figure 26. Reference & altered raw headings of robots during trial.

behavior is more closely observed with exponentially filtered in **Figure 27** and unfiltered data in **Figure 28**. The filtering in **Figure 27** is purely to highlight the trend and separation between the two headings around the noisy values.

The second notable behavior is the difference between robot 0's and robot 1's heading in terms of consistency and stability and is likely a characteristic of the system at large. Specifically, robot 0 begins with a positive heading value and remains positive throughout the trial and contains significant oscillations. However, robot 1's heading begins negative and remains negative but does not contain the high frequency oscillations. This general trend is consistent in many other trials

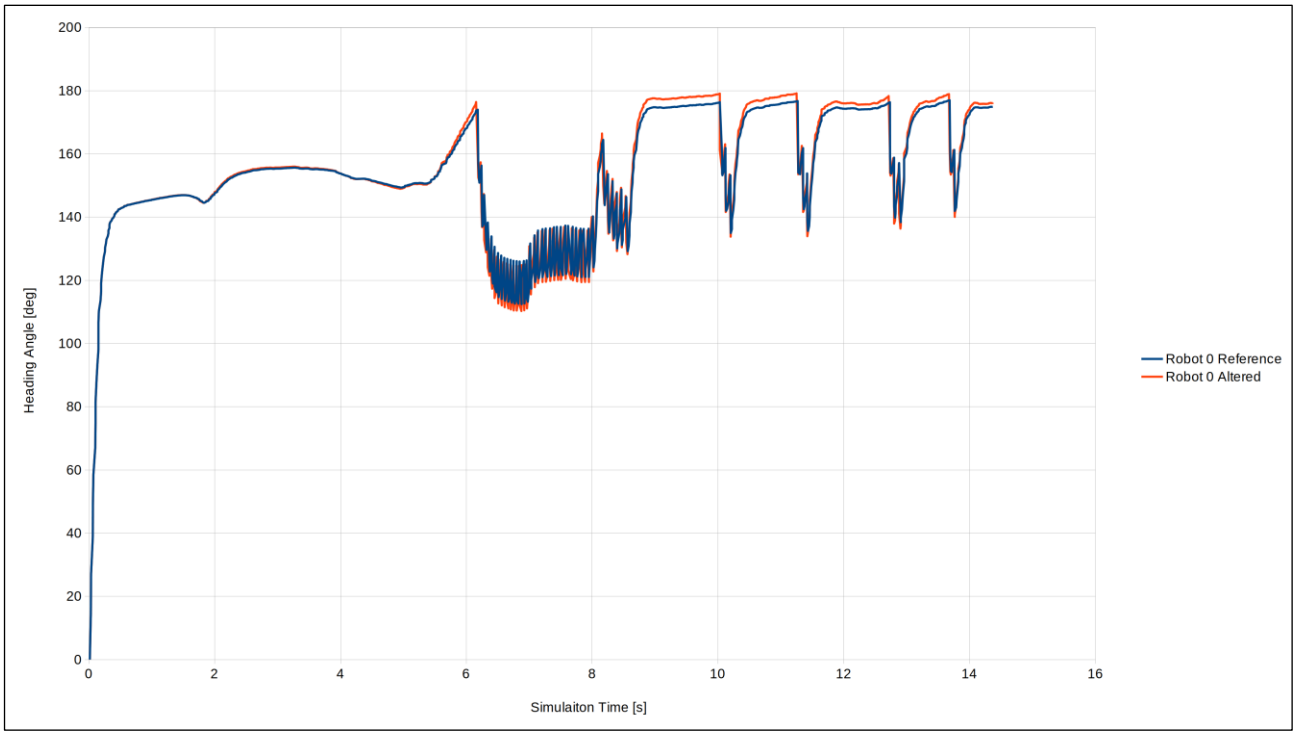

Figure 27. Robot 0 reference & altered headings during trial(exponentially smooth by a factor of 0.1).

performed during testing, although does not hold absolutely. However, it should be considered an error in during development rather than a concrete behavior originating from adherence or convergence. There are many layers to this system from filtering, data processing, and calculation that it is likely somewhere there is a mistake which causes this outcome rather than a property of the proposed solution. While a definitive conclusion is not drawn from this trend, it is worthwhile to consider in future testing.

The last notable behavior is the propagation of heading disturbances between the two robots. Particularly at 10, ~11.5, ~12.5, and ~13.5 seconds into the trial shown in Figure 27. Both robots respond to a disturbance at the same interval in an opposite direction, albeit different magnitudes. Additionally, each robot's response was different between the same, propagated disturbance with robot 0 exhibiting high frequency oscillations and robot 1 a stable adjustment. These can be better viewed in Figure 28 and Figure 30 which contain the difference between the

reference and altered heading with 0 representing no recalculation of the reference from the impedance subsystem.

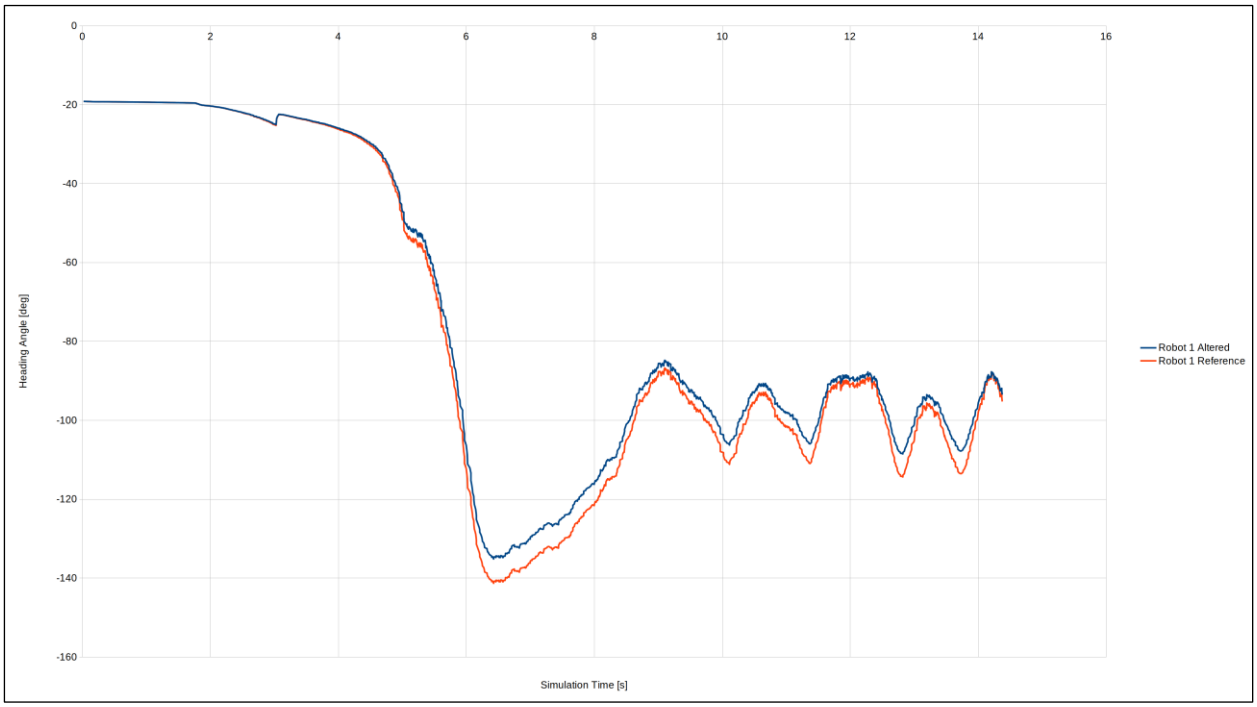

Figure 28. Robot 1 reference & altered headings during trial.

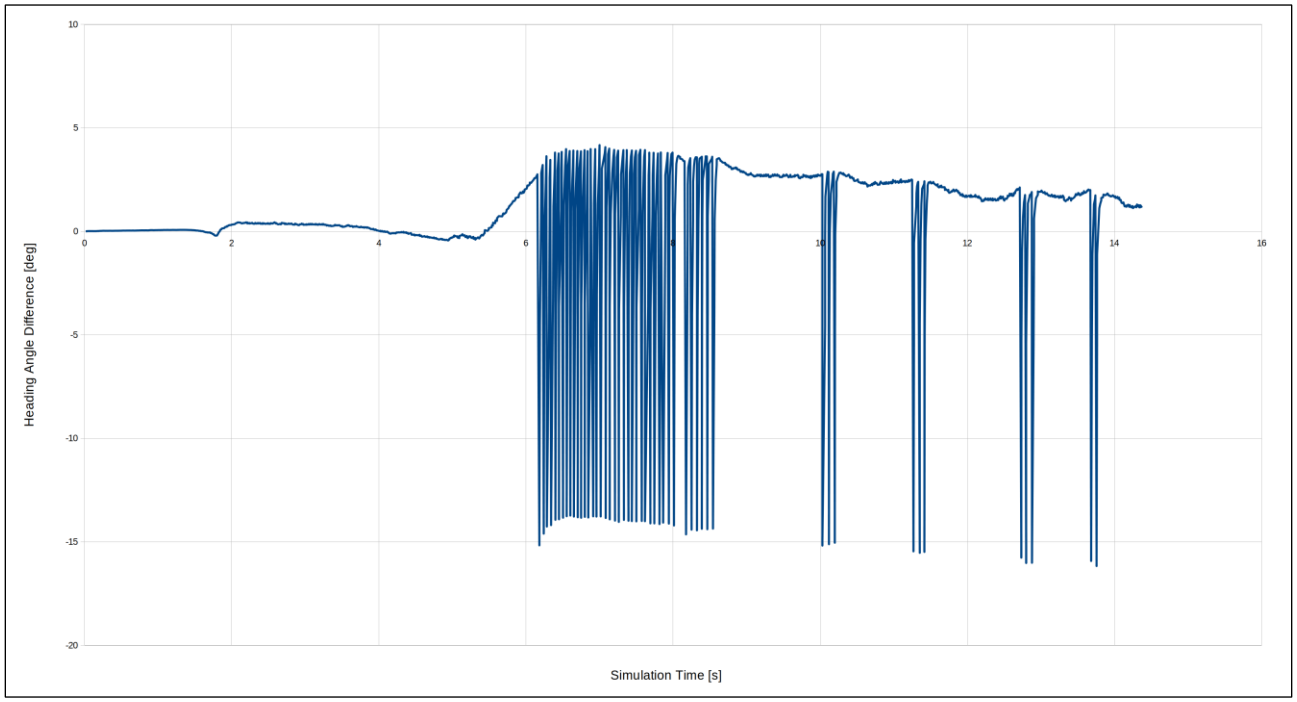

Figure 29. Robot 0 difference between reference & altered heading during trial (exponentially smoothed by a factor of 0.1).

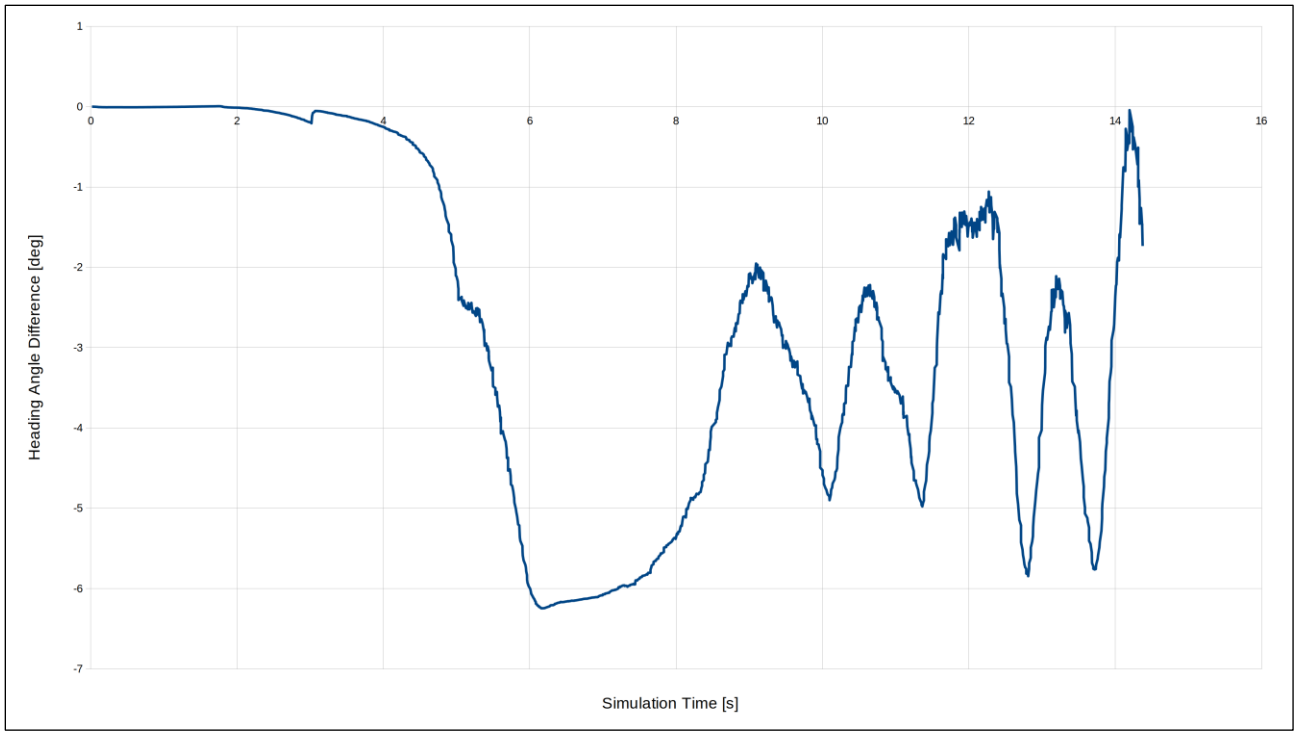

Figure 30. Robot 1 difference between reference & altered heading during trial.

6.4 Overall Simulation Results

Following the development of the Gazebo/ROS simulation, profiling the scalability and system level behavior became necessary. While desirable behaviors were present with one or two robots, it became clear that general observations and a single case would not be sufficient to profile system-level behavior when adding more robots. This endeavor included 10 trials for each of the four cases at 1, 2, 3, 5, and 10 robots which we determined would profile the range of expected physical environments. The results are contained in **Table 4** where each configuration of robots in each case has the 10 trials averaged with accompanying deviation. The dynamic parameters used

Case 1	1 Robot	2 Robots	3 Robots	5 Robots	10 Robots
Success Rate [%]	0.00	0.00	0.00	40.00	0.00
Completion Time [s]	120.16 ± 0.053	120.16 ± 0.033	120.17 ± 0.029	98.30 ± 30.853	120.17 ± 0.018
Agent Travel Distance [m]	21.992 ± 3.9106	33.237 ± 14.7653	38.965 ± 18.3648	41.013 ± 16.5674	58.526 ± 13.9806
Object Travel Distance [m]	8.617 ± 1.7690	21.019 ± 14.2506	18.260 ± 11.8874	25.788 ± 9.9733	40.822 ± 14.0447
Final Object Distance to Goal [m]	7.907 ± 4.1632	16.184 ± 15.6643	13.335 ± 11.8015	10.408 ± 11.6464	28.154 ± 24.7219
Closest Object Distance to Goal [m]	3.599 ± 1.3326	3.342 ± 1.2128	2.486 ± 1.8567	1.635 ± 1.7935	3.740 ± 1.1434
Case 2	1 Robot	2 Robots	3 Robots	5 Robots	10 Robots
Success Rate [%]	0.00	20.00	50.00	20.00	10.00
Completion Time [s]	120.14 ± 0.030	106.76 ± 29.078	75.92 ± 47.303	103.81 ± 34.950	109.94 ± 32.402
Agent Travel Distance [m]	8.315 ± 2.4604	32.973 ± 19.1917	28.026 ± 21.7763	38.542 ± 17.8716	46.503 ± 20.8293
Object Travel Distance [m]	1.861 ± 0.6089	20.341 ± 16.4035	12.436 ± 13.9168	13.270 ± 9.3648	23.536 ± 16.2860
Final Object Distance to Goal [m]	2.261 ± 0.6072	15.375 ± 17.1611	6.745 ± 14.5320	7.088 ± 9.6513	16.277 ± 14.7777
Closest Object Distance to Goal [m]	2.261 ± 0.6072	1.404 ± 0.9285	0.631 ± 0.6258	1.456 ± 0.8222	0.895 ± 0.3672
Case 3	1 Robot	2 Robots	3 Robots	5 Robots	10 Robots
Success Rate [%]	0.00	60.00	30.00	60.00	40.00
Completion Time [s]	120.14 ± 0.040	101.74 ± 21.567	93.81 ± 42.530	63.71 ± 49.127	89.89 ± 48.528
Agent Travel Distance [m]	13.599 ± 5.8535	15.621 ± 4.7814	30.034 ± 19.1831	23.766 ± 19.3916	35.867 ± 23.0862
Object Travel Distance [m]	2.598 ± 1.8299	4.537 ± 1.6780	15.691 ± 12.9933	17.462 ± 19.4639	18.185 ± 16.7887
Final Object Distance to Goal [m]	2.746 ± 0.6136	1.460 ± 1.6449	8.503 ± 12.1237	11.902 ± 18.3005	11.359 ± 16.3350
Closest Object Distance to Goal [m]	2.684 ± 0.5504	1.161 ± 1.1141	0.804 ± 0.4852	0.529 ± 0.3764	0.739 ± 0.5011
Case 4	1 Robot	2 Robots	3 Robots	5 Robots	10 Robots
Success Rate [%]	0.00	30.00	10.00	10.00	30.00
Completion Time [s]	120.14 ± 0.048	96.99 ± 39.232	112.15 ± 25.309	111.52 ± 27.385	93.50 ± 43.028
Agent Travel Distance [m]	12.813 ± 6.6084	25.321 ± 15.6007	38.704 ± 20.6236	40.004 ± 17.3961	31.287 ± 18.5763
Object Travel Distance [m]	4.263 ± 4.0545	8.529 ± 4.7948	21.964 ± 15.4943	19.174 ± 12.3935	19.154 ± 17.6322
Final Object Distance to Goal [m]	5.268 ± 5.0435	2.784 ± 2.2736	16.905 ± 17.0175	11.070 ± 13.1152	11.789 ± 16.9088
Closest Object Distance to Goal [m]	3.142 ± 0.9746	1.065 ± 0.7464	1.941 ± 1.5302	1.783 ± 1.4991	1.204 ± 1.0639

Table 4. System testing data, 10 trials averaged for 1, 2, 3, 5, and 10 robots for each of the four cases.

are found in **Table 3** in section **6.1**. The only reason for variation in the data is the random starting positions between trials within the boundaries created by the four cases.

The behavior of this system is expected to vary with the difficulty of the cases in terms of the success rate and completion time such that increasing the number of bots is anticipated to decrease completion time and increase success rate. Additionally, the following performance metrics are consolidated: “Object Travel Distance” determines path efficiency of the object such that when the object traveled more than 4.24m then undesirable motion occurred while transporting the object. Furthermore, if the “Agent Travel Distance” is significantly higher than the object travel distance, it is likely either the agent disengaged from the object or significant rotation of the object occurred. Performance can be further characterized by the ‘Final Object Distance to Goal’ and the ‘Closest Object Distance to Goal’. The final object distance is the distance between object and goal position when trial time ended. The closest object distance achieved demonstrates how close the object passed by the goal position; even if the trial failed, i.e. it could not be completed within trial time. The object could have nearly missed and, in practical terms, could have been a ‘successful’ transport depending on the operational tolerances.

Across all cases, success rate shows that one robot is unable to transport the object to the goal position within the trial time regardless of the case. This is by design to challenge collaboration in the later trials with more robots. However, there is a clear trend shown by the ‘object distance traveled’ and the ‘closest object distance’ in the single robot trials that the robot is able to orient and begin pushing in the correct direction, but lacks the force necessary to transport the object in time.

During Case 1, in which all robots started in vicinity to the goal position, we can observe that only 5 robots together succeeded. We hypothesized this case to be the most challenging due to the

reliance on the obstacle avoidance terms to fully maneuver around the object. Decreasing distance to goal and increasing agent travel distance indicate that as the robots have to travel far to the pushing point, and are slowed down by pushing the object. In addition, any instability is amplified with adding more robots as shown by this trend and may not coordinate as well with fewer robots.

As mentioned prior and reflected in the data, if the obstacle stiffness and accompanying terms do not overpower the attractor terms, the heading will not be influenced. The result observed in those simulations is that the robots begin pushing on the same side as the goal position and without repositioning on the object or recovering. This behavior can be suppressed through an increase of obstacle stiffness, however if stiffness is chosen too large, it will prevent the robot from ever getting around or achieve stable interaction.

During Case 2, all robots started in the occluded quadrant behind the object - so they were well positioned to push the object immediately. Nevertheless, performance varies. Success rate increases from one, to two, to three robots, but drops again for five and ten. Possibly, as more robots are pushing into one point and hence increasing the likelihood for robots pushing each other away. Consequently, the object is not being moved into the correct direction. As object travel distance for 3 and 5 robots is similar, while agent travel distance differs, we can assume that when 5 or 10 robots interact, heading oscillation might have emerged. In future work we will therefore consider more strategic optimization of adaptive terms. Interestingly, ten robots is able to match the performance of three robots by getting the object within the neighborhood of the goal, but is mostly unable to achieve success.

In the best performing scenario for our work, case 3, robots started from lateral positions to the object. Success rate is best for 2 and 5 robots. Here, the system was able to limit excess object travel in the 2-robot scenario (4.24m shortest) while completion time consistently decreases

from 2, to 3, to 5 robots but increases with 10 robots. This seems to indicate a few fundamental behaviors. When imbalance (relative to starting positions) is present in the system, it is less likely to infinitely push away from the goal position. Secondly, the system is dependent on initial conditions, especially which direction the initial force is coming from. As more robots are introduced into the system the relationship between robots may decouple, as seen with the 5 active robots across the cases: agent travel distance for 3, 5, and 10 robots is simultaneously larger than for two robots, and final object distance to goal increases from 2 to 3 to 5 and 10 robots. Finally, the agents exhibit significant excess or positioning motion potentially by rotating the object or oscillating in free space. This could be balanced out in the future with altered dynamic parameters, however this could bias performance to one case or another depending on the referenced case.

During Case 4, robots were randomly placed within the workspace. Again, the 2-robot scenario seems to be the most stable. As in this case, initial position was not predetermined, 10 trials seem to not suffice for coming to conclusions about system behavior. Nevertheless, even in the random case, with 3, 5, or 10 robots, success was evident.

7 CONCLUSION & FUTURE DIRECTION

After many years of development and time with this system and the consideration of the data presented in the previous sections, several important results deserve recognition and analysis from our work. The first is that contact and indirect communication is necessary to leverage for expanding into environments with greater complexity and uncertainty. Our proposed coupled, dynamic system certainly considers contact from navigation down to mechanical design which better approaches these situations than previously documented methods. Next, a homogenous architecture for MAS provides necessary benefits and simplifications compared to popular leader-follower methods when integrating contact design. Specifically, with every robot able to act upon similarly measured information and decision-making processes, adherence calculates an altered heading without any adjustment or hesitation. As explored in the previous sections, any latency or hesitation could introduce instability or undesirable interaction which does not benefit the overall object transportation objective. Thirdly, from a mobile robot standpoint, a reference trajectory attractor dynamics navigation method introduces the least architectural latency compared to the presented examples by calculating a series of stable state attractors in real time. However, complex, often nonlinear, calculations are required which introduces calculation latency on modern microcontrollers for a physical system. In the future this could be remedied by a simplification of calculation or more efficient processors. Lastly, and most importantly, the proposed coupled dynamic system operates in a expected capacity following the analysis from sections **6.3** and **6.4**. While improvements are certainly required for the system to eventually see a physical or potentially commercial application, clear routes are available from the developed foundation.

In the future this work will be iterated and improved through two avenues, within the simulation and physical validation. The first logical step for the simulation is Documenting and

exploring the analytical implications of a second order trajectory planner and physical interaction controller. While stability is acknowledged in our work we recognize that additional analysis may lead to a more stable system through a specific set of dynamic bounds. Furthermore, we will remove reliance on global information or geometric profiles. We think a method could exist with the addition of LIDAR or rgb-d cameras alongside the implemented haptic information. This way the agent could recognize the object which requires manipulation and where to place attractor or repeller points online. Lastly in the simulation, with modern progress into learning methods the inclusion of a learning method such as reinforcement learning, neural network, or possibly fuzzy methods could augment the adaptability of both convergence and adherence.

Physical robots also hold significant promise to support the findings of the simulation and results documented above. While some details and a few fundamental differences must be investigated such as the different force measurement methods, it is anticipated that a similar conclusion would arise between the simulation and its physical implementation. However, the crux that will underpin any future efforts to bring a physical system is stability as was a great challenge in this phase of the project.

8 REFERENCES

[1] E. Ackerman, “Astrobee Will Find Astronauts’ Lost Socks,” *IEE Spectrum*, 2021. https://spectrum.ieee.org/astrobee-nasa-gateway.

[2] G. S. Conceic, “Perception-Driven Multi-Robot Formation Control,” pp. 1851–1856, 2013.

[3] M. Zhang, Y. Shen, Q. Wang, and Y. Wang, “Dynamic artificial potential field based multi-robot formation control,” *2010 IEEE Int. Instrum. Meas. Technol. Conf. I2MTC 2010 - Proc.*, vol. 2, no. 1, pp. 1530–1534, 2010, doi: 10.1109/IMTC.2010.5488238.

[4] J. S. Dalfior and R. F. Vassallo, “Nonlinear formation control for a cooperative load pushing,” *Proc. IEEE Int. Conf. Ind. Technol.*, pp. 1439–1444, 2010, doi: 10.1109/ICIT.2010.5472493.

[5] G. Lee and D. Chwa, “Decentralized behavior-based formation control of multiple robots considering obstacle avoidance,” *Intell. Serv. Robot.*, vol. 11, no. 1, pp. 127–138, 2018, doi: 10.1007/s11370-017-0240-y.

[6] H. Ebel and P. Eberhard, “Non-Prehensile Cooperative Object Transportation with Omnidirectional Mobile Robots : Organization , Control , Simulation , and Experimentation,” 2021.

[7] R. Parasuraman, J. Kim, S. Luo, and B. C. Min, “Multipoint Rendezvous in Multirobot Systems,” *IEEE Trans. Cybern.*, vol. 50, no. 1, pp. 310–323, 2020, doi: 10.1109/TCYB.2018.2868870.

[8] R. Soares, E. Bicho, T. Machado, and W. Erlhagen, “Object transportation by multiple mobile robots controlled by attractor dynamics: Theory and implementation,” *IEEE Int.*

Conf. Intell. Robot. Syst., pp. 937–944, 2007, doi: 10.1109/IROS.2007.4399019.

[9] T. Sun, H. Liu, Y. Yao, T. Li, and Z. Cheng, "Distributed adaptive formation tracking control under fixed and switching topologies: Application on general linear multi-agent systems," *Symmetry (Basel).*, vol. 13, no. 6, 2021, doi: 10.3390/sym13060941.

[10] E. Tuci, M. H. M. Alkilabi, and O. Akanyeti, "Cooperative object transport in multi-robot systems: A review of the state-of-the-art," *Front. Robot. AI*, vol. 5, no. MAY, 2018, doi: 10.3389/frobt.2018.00059.

[11] R. S. Melo, D. G. Macharet, and M. F. M. Campos, "Multi-object Transportation Using a Mobile Robot," *Proc. - 12th LARS Lat. Am. Robot. Symp. 3rd SBR Brazilian Robot. Symp. LARS-SBR 2015 - Part Robot. Conf. 2015*, no. i, pp. 234–239, 2016, doi: 10.1109/LARS-SBR.2015.17.

[12] B. R. Fajen and W. H. Warren, "Behavioral Dynamics of Steering, Obstacle Avoidance, and Route Selection," *J. Exp. Psychol. Hum. Percept. Perform.*, vol. 29, no. 2, pp. 343–362, 2003, doi: 10.1037/0096-1523.29.2.343.

[13] E. Bach, K. Pandey, B. Russ, and J. M. Youm, "Force Sensing Mobile Robot Project," 2022.

[14] B. K. Patle, G. Babu L, A. Pandey, D. R. K. Parhi, and A. Jagadeesh, "A review: On path planning strategies for navigation of mobile robot," *Defence Technology*, vol. 15, no. 4. China Ordnance Society, pp. 582–606, Aug. 01, 2019, doi: 10.1016/j.dt.2019.04.011.

[15] M. Hoy, A. S. Matveev, and A. V. Savkin, "Algorithms for collision-free navigation of mobile robots in complex cluttered environments: A survey," *Robotica*, vol. 33, no. 3, pp. 463–497, Mar. 2015, doi: 10.1017/S0263574714000289.

[16] M. N. A. Wahab, S. Nefti-Meziani, and A. Atyabi, “A comparative review on mobile robot path planning: Classical or meta-heuristic methods?,” *Annu. Rev. Control*, vol. 50, no. October, pp. 233–252, 2020, doi: 10.1016/j.arcontrol.2020.10.001.

[17] A. C. Hernandes, H. B. Guerrero, M. Becker, J. S. Jokeit, and G. Schöner, “A comparison between reactive potential fields and Attractor Dynamics,” *2014 IEEE 5th Colomb. Work. Circuits Syst. CWCAS 2014 - Conf. Proc.*, no. 3, 2014, doi: 10.1109/CWCAS.2014.6994609.

[18] A. A. Ravankar, A. Ravankar, T. Emaru, and Y. Kobayashi, “HPPRM: Hybrid Potential Based Probabilistic Roadmap Algorithm for Improved Dynamic Path Planning of Mobile Robots,” *IEEE Access*, vol. 8, pp. 221743–221766, 2020, doi: 10.1109/ACCESS.2020.3043333.

[19] C. E. Luis, M. Vukosavljev, and A. P. Schoellig, “Online Trajectory Generation with Distributed Model Predictive Control for Multi-Robot Motion Planning,” pp. 1–8, 2019.

[20] C. Shen and Y. Shi, “Distributed implementation of nonlinear model predictive control for AUV trajectory tracking,” *Automatica*, vol. 115, p. 108863, 2020, doi: 10.1016/j.automatica.2020.108863.

[21] M. Zhu, L. Ye, and X. Ma, “Estimation-Based Quadratic Iterative Learning Control for Trajectory Tracking of Robotic Manipulator with Uncertain Parameters,” *IEEE Access*, vol. 8, pp. 43122–43133, 2020, doi: 10.1109/ACCESS.2020.2977687.

[22] I. Kim, S. H. Nengroo, and D. Har, “Mobile Robot with LiDAR,” no. 2020, pp. 148–154, 2021.

[23] K. S. Kim, A. S. Kwok, G. C. Thomas, and L. Sentis, “Fully omnidirectional compliance in mobile robots via drive-torque sensor feedback,” *IEEE Int. Conf. Intell. Robot. Syst.*, no. Iros, pp. 4757–4763, 2014, doi: 10.1109/IROS.2014.6943239.

[24] M. Kollmitz, D. Buscher, T. Schubert, and W. Burgard, “Whole-Body Sensory Concept for Compliant Mobile Robots,” *Proc. - IEEE Int. Conf. Robot. Autom.*, pp. 5429–5435, 2018, doi: 10.1109/ICRA.2018.8460510.

[25] K. Bodie *et al.*, “Active Interaction Force Control for Contact-Based Inspection with a Fully Actuated Aerial Vehicle,” *IEEE Trans. Robot.*, vol. 37, no. 3, pp. 709–722, 2021, doi: 10.1109/TRO.2020.3036623.

[26] M. Tsuji and T. Murakami, “Collaborative Transport by Mecanum Mobile Robots using Reaction Torque Observer,” pp. 185–190, 2020, doi: 10.1109/amc44022.2020.9244326.

[27] Z. D. Wang, K. Fukaya, Y. Hirata, and K. Kosuge, “Control passive mobile robots for object transportation braking torque analysis and motion control,” *Proc. - IEEE Int. Conf. Robot. Autom.*, no. April, pp. 2874–2879, 2007, doi: 10.1109/ROBOT.2007.363907.

[28] T. Manderson, S. Wapnick, D. Meger, and G. Dudek, “Learning to Drive off Road on Smooth Terrain in Unstructured Environments Using an On-Board Camera and Sparse Aerial Images,” *Proc. - IEEE Int. Conf. Robot. Autom.*, pp. 1263–1269, 2020, doi: 10.1109/ICRA40945.2020.9196879.

[29] D. Chatziparaschis, M. G. Lagoudakis, and P. Partsinevelos, “Aerial and ground robot collaboration for autonomous mapping in search and rescue missions,” *Drones*, vol. 4, no. 4, pp. 1–24, 2020, doi: 10.3390/DRONES4040079.

[30] D. Sakai, H. Fukushima, and F. Matsuno, “Flocking for Multirobots Without Distinguishing Robots and Obstacles,” *IEEE Trans. Control Syst. Technol.*, vol. 25, no. 3, pp. 1019–1027, 2017, doi: 10.1109/TCST.2016.2581148.

[31] P. Shi and B. Yan, “A Survey on Intelligent Control for Multiagent Systems,” *IEEE Trans. Syst. Man, Cybern. Syst.*, vol. 51, no. 1, pp. 161–175, 2021, doi: 10.1109/TSMC.2020.3042823.

[32] Y. Yang, N. Xiong, Y. C. Nak, and X. Défago, “A decentralized and adaptive flocking algorithm for autonomous mobile robots,” *Proc. - 3rd Int. Conf. Grid Pervasive Comput. Symp. GPC 2008*, pp. 262–268, 2008, doi: 10.1109/GPC.WORKSHOPS.2008.18.

[33] M. Yan, J. V. Nickerson, and G. Jing, “Multi-robot aggregation strategies with limited communication,” *IEEE Int. Conf. Intell. Robot. Syst.*, pp. 2691–2696, 2006, doi: 10.1109/IROS.2006.281991.

[34] P. Oikonomou and S. Pappas, “Decentralized bioinspired non-discrete model for autonomous swarm aggregation dynamics,” *Appl. Sci.*, vol. 10, no. 3, pp. 1–18, 2020, doi: 10.3390/app10031067.

[35] S. Zhao, D. V. Dimarogonas, Z. Sun, and D. Bauso, “A General Approach to Coordination Control of Mobile Agents with Motion Constraints,” *IEEE Trans. Automat. Contr.*, vol. 63, no. 5, pp. 1509–1516, May 2018, doi: 10.1109/TAC.2017.2750924.

[36] A. J. Ijspeert, J. Nakanishi, H. Hoffmann, P. Pastor, and S. Schaal, “Dynamical movement primitives: Learning attractor models for motor behaviors,” *Neural Comput.*, vol. 25, no. 2, pp. 328–373, 2013, doi: 10.1162/NECO_a_00393.

[37] E. Bicho and S. Monteiro, "Formation control for multiple mobile robots: A non-linear attractor dynamics approach," *IEEE Int. Conf. Intell. Robot. Syst.*, vol. 2, pp. 2016–2022, 2003, doi: 10.1109/iros.2003.1248953.

[38] S. Monteiro and E. Bicho, "Attractor dynamics approach to formation control: Theory and application," *Auton. Robots*, vol. 29, no. 3–4, pp. 331–355, 2010, doi: 10.1007/s10514-010-9198-8.

[39] T. Machado, T. Malheiro, S. Monteiro, W. Erlhagen, and E. Bicho, "Attractor dynamics approach to joint transportation by autonomous robots: theory, implementation and validation on the factory floor," *Auton. Robots*, vol. 43, no. 3, pp. 589–610, 2019, doi: 10.1007/s10514-018-9729-2.

[40] S. Monteiro and E. Bicho, "A dynamical systems approach to behavior-based formation control," *Proc. - IEEE Int. Conf. Robot. Autom.*, vol. 3, pp. 2606–2611, 2002, doi: 10.1109/robot.2002.1013624.

[41] B. R. Fajen and W. H. Warren, "Behavioral dynamics of intercepting a moving target," *Exp. Brain Res.*, vol. 180, no. 2, pp. 303–319, 2007, doi: 10.1007/s00221-007-0859-6.

[42] W. H. Warren, "The dynamics of perception and action," *Psychol. Rev.*, vol. 113, no. 2, pp. 358–389, 2006, doi: 10.1037/0033-295X.113.2.358.

[43] K. Kronander and A. Billard, "Passive Interaction Control With Dynamical Systems," *IEEE Robot. Autom. Lett.*, vol. 1, no. 1, pp. 106–113, 2016, doi: 10.1109/LRA.2015.2509025.

[44] M. Khoramshahi and A. Billard, "A dynamical system approach for detection and reaction to human guidance in physical human–robot interaction," *Auton. Robots*, vol. 44, no. 8, pp.

1411–1429, 2020, doi: 10.1007/s10514-020-09934-9.

[45] M. Ruderman, “On switching between motion and force control,” *27th Mediterr. Conf. Control Autom. MED 2019 - Proc.*, no. 2, pp. 445–450, 2019, doi: 10.1109/MED.2019.8798545.

[46] N. Hogan, “Impedance control: An approach to manipulation: Part I-Theory,” *J. Dyn. Syst. Meas. Control. Trans. ASME*, vol. 107, no. 1, pp. 1–7, 1985, doi: 10.1115/1.3140701.

[47] H. Ye, S. Jiang, and J. Wang, “Research on Contact Force Control of Grinding Robot based on Adaptive Impedance Control,” *IEEE Inf. Technol. Networking, Electron. Autom. Control Conf. ITNEC 2021*, pp. 290–293, 2021, doi: 10.1109/ITNEC52019.2021.9586992.

[48] H. Liu, W. Lu, X. Zhu, X. Wang, and B. Liang, “Force tracking impedance control with moving target,” *2017 IEEE Int. Conf. Robot. Biomimetics, ROBIO 2017*, vol. 2018-Janua, no. 1, pp. 1–6, 2018, doi: 10.1109/ROBIO.2017.8324608.

[49] M. H. Hamedani, H. Sadeghian, M. Zekri, F. Sheikholeslam, and M. Keshmiri, “Intelligent Impedance Control using Wavelet Neural Network for dynamic contact force tracking in unknown varying environments,” *Control Eng. Pract.*, vol. 113, no. November 2020, p. 104840, 2021, doi: 10.1016/j.conengprac.2021.104840.

[50] P. Song, Y. Yu, and X. Zhang, “A Tutorial Survey and Comparison of Impedance Control on Robotic Manipulation,” *Robotica*, vol. 37, no. 5, pp. 801–836, 2019, doi: 10.1017/S0263574718001339.

[51] J. E. Colgate and N. Hogan, “Robust control of dynamically interacting systems,” *Int. J. Control*, vol. 48, no. 1, pp. 65–88, 1988, doi: 10.1080/00207178808906161.

[52] J. E. Colgate, “The Control of Dynamically Interacting Systems,” *Robotics and Autonomous Systems*, vol. 1, no. 3. pp. 1–14, 1988, [Online]. Available: http://ezproxy.net.ucf.edu/login?url=http://search.proquest.com/docview/304999885?accountid=10003%5Cnhttp://sfx.fcla.edu/ucf?url_ver=Z39.88-2004&rft_val_fmt=info:ofi/fmt:kev:mtx:dissertation&genre=dissertations+&+theses&sid=ProQ:ProQuest+Dissertations+&+T.

[53] N. Figueroa, “From High-Level to Low-Level Robot Learning of Complex Tasks: Leveraging Priors, Metrics and Dynamical Systems,” 2019.

[54] J. Duan, Y. Gan, M. Chen, and X. Dai, “Adaptive variable impedance control for dynamic contact force tracking in uncertain environment,” *Rob. Auton. Syst.*, vol. 102, pp. 54–65, 2018, doi: 10.1016/j.robot.2018.01.009.

[55] H. Cao, X. Chen, Y. He, and X. Zhao, “Dynamic Adaptive Hybrid Impedance Control for Dynamic Contact Force Tracking in Uncertain Environments,” *IEEE Access*, vol. 7, pp. 83162–83174, 2019, doi: 10.1109/ACCESS.2019.2924696.

[56] K. Kronander and A. Billard, “Stability Considerations for Variable Impedance Control,” *IEEE Trans. Robot.*, vol. 32, no. 5, pp. 1298–1305, 2016, doi: 10.1109/TRO.2016.2593492.

[57] “Complexity - 2008 - Halley - Classification of emergence and its relation to self-organization.pdf.” .

[58] R. Buckminster Fuller, “Tensile-Integrity Structures. US3063521 Patent,” 1962.

[59] D. E. Ingber, “Tensegrity I. Cell structure and hierarchical systems biology,” *J. Cell Sci.*, vol. 116, no. 7, pp. 1157–1173, Apr. 2003, doi: 10.1242/jcs.00359.

[60] L. Wu, M. J. de Andrade, T. Brahme, Y. Tadesse, and R. H. Baughman, "A deformable robot with tensegrity structure using nylon artificial muscle," Apr. 2016, no. April 2016, p. 97993K, doi: 10.1117/12.2219641.

[61] S. Sumi, P. Schorr, V. Böhm, and K. Zimmermann, *Dynamic Analysis of a Compliant Tensegrity Structure for the Use in a Gripper Application*. Springer International Publishing.

[62] J. Bruce, K. Caluwaerts, A. Iscen, A. P. Sabelhaus, and V. Sunspiral, "Design and Evolution of a Modular Tensegrity Robot Platform," pp. 3483–3489, 2014.

[63] K. Caluwaerts, J. Bruce, J. M. Friesen, and V. SunSpiral, "State estimation for tensegrity robots," in *2016 IEEE International Conference on Robotics and Automation (ICRA)*, May 2016, pp. 1860–1865, doi: 10.1109/ICRA.2016.7487331.

[64] P. Caldeira, S. T. Fonseca, A. Paulo, J. Infante, and D. Araújo, "Linking Tensegrity to Sports Team Collective Behaviors: Towards the Group-Tensegrity Hypothesis," *Sport. Med. - Open*, vol. 6, no. 1, 2020, doi: 10.1186/s40798-020-00253-y.

[65] E. Ferrante, A. E. Turgut, C. Huepe, A. Stranieri, C. Pinciroli, and M. Dorigo, "Self-organized flocking with a mobile robot swarm: A novel motion control method," *Adapt. Behav.*, vol. 20, no. 6, pp. 460–477, 2012, doi: 10.1177/1059712312462248.

[66] N. Mathew, S. L. Smith, and S. L. Waslander, "Multirobot rendezvous planning for recharging in persistent tasks," *IEEE Trans. Robot.*, vol. 31, no. 1, pp. 128–142, 2015, doi: 10.1109/TRO.2014.2380593.

[67] Z. Qiao, J. Zhang, X. Qu, and J. Xiong, "Dynamic Self-Organizing Leader-Follower

Control in a Swarm Mobile Robots System under Limited Communication," *IEEE Access*, vol. 8, pp. 53850–53856, 2020, doi: 10.1109/ACCESS.2020.2980778.

[68] A. Tsiamis, C. P. Bechlioulis, G. C. Karras, and K. J. Kyriakopoulos, "Decentralized object transportation by two nonholonomic mobile robots exploiting only implicit communication," *Proc. - IEEE Int. Conf. Robot. Autom.*, vol. 2015-June, no. June, pp. 171–176, 2015, doi: 10.1109/ICRA.2015.7138996.

[69] B. R. Fajen, W. H. Warren, S. Temizer, and L. P. Kaelbing, "A dynamical model of visually-guided steering, obstacle avoidance, and route selection," *Int. J. Comput. Vis.*, vol. 54, no. 1–3, pp. 13–34, 2003, doi: 10.1023/a:1023701300169.

[70] O. Ma, "AEEM 6117 Intelligent Robots: Impedance Control." 2022.

[71] G. Ritter, "Open Base." [Online]. Available: https://github.com/GuiRitter/OpenBase.